



BILINGUAL
PUBLISHING CO.
Pioneer of Global Academics Since 1984

Journal of Electronic & Information Systems

Volume 4 • Issue 2 • October 2022 ISSN 2661-3204 (Online)





**BILINGUAL
PUBLISHING CO.**
Pioneer of Global Academics Since 1984

Editor-in-Chief

Prof. Xinggang Yan

University of Kent, United Kingdom

Editorial Board Members

| | |
|--------------------------------------|---|
| Chong Huang, United States | Husam Abduldaem Mohammed, Iraq |
| Yoshifumi Manabe, Japan | Neelamadhab Padhy, India |
| Hao Xu, United States | Baofeng Ji, China |
| Shicheng Guo, United States | Maxim A. Dulebenets, United States |
| Diego Real Mañez, Spain | Jafar Ramadhan Mohammed, Iraq |
| Senthil Kumar Kumaraswamy, India | Shitharth Selvarajan, India |
| Santhan Kumar Cherukuri, India | Schekeb Fateh, Switzerland |
| Asit Kumar Gain, Australia | Alexandre Jean Rene Serres, Brazil |
| Sedigheh Ghofrani, Iran | Dadmehr Rahbari, Iran |
| Lianggui Liu, China | Jun Shen, China |
| Saleh Mobayen, Iran | Yuan Tian, China |
| Ping Ding, China | Abdollah Doosti-Aref, Iran |
| Youqiao Ma, Canada | Fei Wang, China |
| M.M. Kamruzzaman, Bangladesh | Xiaofeng Yuan, China |
| Seyed Saeid Moosavi Anchehpoli, Iran | Kamarulzaman Kamarudin, Malaysia |
| Sayed Alireza Sadrossadat, Iran | Tajudeen Olawale Olasupo, United States |
| Sasmita Mohapatra, India | Md. Mahbubur Rahman, Korea |
| Akram Sheikhi, Iran | Héctor F. Migallón, Spain |

Volume 4 Issue 2 • October 2022 • ISSN 2661-3204 (Online)

Journal of Electronic & Information Systems

Editor-in-Chief
Prof. Xinggang Yan



**BILINGUAL
PUBLISHING CO.**
Pioneer of Global Academics Since 1984



Contents

Articles

- 1** **New Approach to Observer-Based Finite-Time H_∞ Control of Discrete-Time One-Sided Lipschitz Systems with Uncertainties**
Xinyue Tang Yali Dong Meng Liu
- 10** **Monitoring Heart Rate Variability Based on Self-powered ECG Sensor Tag**
Nhat Minh Tran Ngoc-Giao Pham Thang Viet Tran
- 21** **Deploying a Deep Learning-based Application for an Efficient Thermal Energy Storage Air-Conditioning (TES-AC) System: Design Guidelines**
Mirza Rayana Sanzana Mostafa Osama Mostafa Abdulrazic Jing Ying Wong Chun-Chieh Yip

ARTICLE

New Approach to Observer-Based Finite-Time H_∞ Control of Discrete-Time One-Sided Lipschitz Systems with Uncertainties

Xinyue Tang Yali Dong* Meng Liu

School of Mathematical Sciences, Tiangong University, Tianjin, 300387, China

ARTICLE INFO

Article history

Received: 30 April 2022

Revised: 12 July 2022

Accepted: 29 July 2022

Published Online: 5 September 2022

Keywords:

Finite-time H_∞ boundedness

Discrete-time systems

One-sided Lipschitz system

Observer-based control

ABSTRACT

This paper investigates the finite-time H_∞ control problem for a class of nonlinear discrete-time one-sided Lipschitz systems with uncertainties. Using the one-sided Lipschitz and quadratically inner-bounded conditions, the authors derive less conservative criterion for the controller design and observer design. A new criterion is proposed to ensure the closed-loop system is finite-time bounded (FTB). The sufficient conditions are established to ensure the closed-loop system is H_∞ finite-time bounded (H_∞ FTB) in terms of matrix inequalities. The controller gains and observer gains are given. A numerical example is provided to demonstrate the effectiveness of the proposed results.

1. Introduction

It is widely accepted that a large percentage of systems are nonlinear in nature. As a result, many studies on nonlinear systems have been conducted in the previous several decades. However, most of the times, nonlinearities discussed in these papers focus on traditional Lipschitz condition^[1-4]. It is worth noting that the Lipschitz nonlinear system in the above literature is usually only applicable to some nonlinear systems with sufficiently small Lip-

schitz constant. The so-called one-sided Lipschitz nonlinear system was developed to overcome this difficulty. Later, quadratically inner-bounded condition was proposed by Abbaszadeh and Marquez^[5]. It is worth noting that the traditional Lipschitz system is a special case of one-sided Lipschitz system and quadratic inner bounded system. Therefore, nonlinear systems satisfying quadratic inner boundedness condition and one-sided Lipschitz condition describe a wider class of nonlinear systems.

In practical engineering, many control problems can

*Corresponding Author:

Yali Dong,

School of Mathematical Sciences, Tiangong University, Tianjin, 300387, China;

Email: dongyl@vip.sina.com

DOI: <https://doi.org/10.30564/jeis.v4i2.4684>

Copyright © 2022 by the author(s). Published by Bilingual Publishing Co. This is an open access article under the Creative Commons Attribution-NonCommercial 4.0 International (CC BY-NC 4.0) License. (<https://creativecommons.org/licenses/by-nc/4.0/>).

be summed up as H_∞ standard control problems: interference suppression problem, tracking problem, and robust stability problem. Because of its practical importance, the H_∞ control problem has always been an important research topic. The main purpose of H_∞ control is based on reducing the influence of external disturbance input on the adjustable output of the system. In order to ensure the required robust stability, some results have been obtained on the design of H_∞ control [6-11]. This control is usually available on the assumption that the entire state is accessible. However, in numerous cases, this assumption is invalid, so it is very important to construct an observer that can provide the estimated value of the system state [12]. In recent years, the observer-based control has attracted the attention of researchers, and some results have been obtained [13,14].

Moreover, in some practical cases, the system state cannot exceed a defined boundary within a finite time interval. Hence, the finite-time transient performance should be considered. Recently, finite-time stability and H_∞ control problems have gradually become a well-researched topic and have been applied to many systems [15-18]. In 2020, Wang J X et al. [15] considered the problem of robust finite-time stabilization for uncertain discrete-time linear singular systems. Feng T et al. [16] studied the problem of finite time stability and stabilization for fractional-order switched singular continuous-time system. Zhang T L et al. [17] looked at the finite-time stability and stabilization for linear discrete stochastic systems.

However, so far, the problem of observer-based finite-time H_∞ control for discrete-time one-sided Lipschitz systems have not been fully addressed, which leads to the main purpose of our research.

In this paper, the observer-based finite-time H_∞ controller for nonlinear discrete-time system with uncertainties is studied. We design the observer and observer-based controller. Using Lyapunov function approach and some lemmas, we obtain the criterion of H_∞ FTB for the closed-loop system. Finally, the validity of the proposed method is demonstrated by a numerical example.

This paper is organized as follows. Section 2 covers some preliminary information as well as the problem statement. In Section 3, the sufficient conditions of FTB an H_∞ FTB for nonlinear discrete-time systems are established. In Section 4, a numerical example is presented. Conclusions are given in Section 5.

Notations R^n denotes the n -dimensional Euclidean space. * denotes a block of symmetry. $B < 0(B > 0)$ denotes the matrix B is a negative definite (positive definite) symmetric matrix. We define $He(S) = S + S^T$. $\lambda_{\max}(\cdot)$ and $\lambda_{\min}(\cdot)$ denotes the maximum eigenvalue and minimum eigen-

value of a matrix respectively. $\langle \cdot \rangle$ is inner product in the space R^n , i.e. given $x, y \in R^n$, then $\langle x, y \rangle = x^T y$. \mathbb{N} denotes the non-negative integer set.

2. Problem Formulation

Consider the following uncertain one-sided Lipschitz discrete-time system:

$$\begin{cases} x_{k+1} = (A + \Delta A(k))x_k + g(x_k) + Bu_k + w_k, \\ y_k = (C + \Delta C(k))x_k, \\ z_k = Ex_k + Fw_k, \end{cases} \quad (1)$$

where $x_k \in R^n$ is the n -dimensional state vector, $y_k \in R^l$ is the output measurement, and $u_k \in R^m$ is the control input. $z_k \in R^q$ is the control output. The disturbance $w_k \in R^p$ satisfies:

$$\sum_{k=0}^N w_k^T w_k \leq d^2, d \geq 0. \quad (2)$$

A, B, C, E and F are known real constant matrices. $\Delta A(k)$ and $\Delta C(k)$ are time-varying matrices, which are assumed to be of the form:

$$\Delta A(k) = M_1 \Delta_1(k) N_1, \quad \Delta C(k) = M_2 \Delta_2(k) N_2, \quad (3)$$

where M_1, M_2, N_1 and N_2 are known real constant matrices, and $\Delta_i(k) (i=1,2)$ are the unknown time-varying matrix-valued function subject to the following conditions:

$$\Delta_i^T(k) \Delta_i(k) \leq I, \quad \forall k \in \mathbb{N}, \quad i=1,2. \quad (4)$$

$g(x_k)$ is a nonlinear function satisfying the following assumptions.

Assumption 1 [19] $g(x)$ verifies the one-sided Lipschitz condition:

$$\langle g(x) - g(\hat{x}), x - \hat{x} \rangle \leq \rho \|x - \hat{x}\|^2, \quad \forall x, \hat{x} \in R^n, \quad (5)$$

where ρ is the so-called one sided Lipschitz constant.

Assumption 2 [19] $g(x)$ verifies the quadratic inner-bounded condition:

$$\|g(x) - g(\hat{x})\|^2 \leq \beta \|x - \hat{x}\|^2 + \alpha \langle g(x) - g(\hat{x}), x - \hat{x} \rangle, \quad \forall x, \hat{x} \in R^n, \quad (6)$$

where α and β are known constants.

Remark 1 Different from the traditional Lipschitz condition, constant ρ , α and β in the nonlinearity considered here can be negative, positive or zero.

In this paper, we construct the following state observer-based controller:

$$\begin{cases} \hat{x}_{k+1} = A\hat{x}_k + g(\hat{x}_k) + Bu_k + L(y_k - C\hat{x}_k), \\ u_k = -K\hat{x}_k, \end{cases} \quad (7)$$

where \hat{x}_k is the estimate of x_k , K and L are the controller and observer gains, respectively, to be designed.

Let $e_k = x_k - \hat{x}_k$. Then we have:

$$\begin{aligned} e_{k+1} &= x_{k+1} - \hat{x}_{k+1} \\ &= (A - LC)e_k + (\Delta A - L\Delta C)x_k + \tilde{g}(x_k, \hat{x}_k) + w_k, \end{aligned}$$

where $\tilde{g}(x_k, \hat{x}_k) = g(x_k) - g(\hat{x}_k)$.

Let $\bar{x}_k = [x_k^T \ e_k^T]^T$. The closed-loop system can be written as:

$$\bar{x}_{k+1} = \bar{A}\bar{x}_k + \bar{g}(\bar{x}_k) + \bar{I}w_k, \quad (8)$$

where,

$$\bar{A} = \begin{bmatrix} A + \Delta A - BK & BK \\ \Delta A - L\Delta C & A - LC \end{bmatrix}, \quad (9)$$

$$\bar{g}(\bar{x}_k) = \begin{bmatrix} g(x_k) \\ \tilde{g}(x_k, \hat{x}_k) \end{bmatrix}, \quad \bar{I} = \begin{bmatrix} I \\ I \end{bmatrix}.$$

The following definitions and some useful lemmas are introduced to establish our main results.

Definition 1 (FTB) The closed-loop system (8) is said to be FTB with respect to (c_1, c_2, N, \bar{R}) , where $0 < c_1 < c_2$, $\bar{R} > 0$, if

$$\bar{x}_0^T \bar{R} \bar{x}_0 \leq c_1 \Rightarrow \bar{x}_k^T \bar{R} \bar{x}_k < c_2, \forall k \in \{1, 2, \dots, N\}. \quad (10)$$

Definition 2 (H_∞ FTB) The closed-loop system (8) is said to be H_∞ FTB with respect to $(c_1, c_2, N, \bar{R}, \gamma)$, where $0 < c_1 < c_2$, $\bar{R} > 0$, if the system (8) is FTB with respect to (c_1, c_2, N, \bar{R}) and under the zero-initial condition the following condition is satisfied

$$\sum_{k=0}^N z_k^T z_k < \gamma^2 \sum_{k=0}^N w_k^T w_k, \quad (11)$$

where γ is a prescribed positive scalar.

Lemma 1 ^[18] Given constant matrices X_1, X_2 and X_3 , where $X_1 = X_1^T$, $X_2 = X_2^T > 0$, then we obtain that $X_1 +$

$$X_3^T X_2^{-1} X_3 < 0 \text{ if and only if } \begin{bmatrix} X_1 & X_3^T \\ X_3 & -X_2 \end{bmatrix} < 0.$$

Lemma 2 ^[10] Let D, S and Δ be real matrices with appropriate dimensions and $\Delta^T \Delta \leq I$, the following inequality holds:

$$D\Delta S + S^T \Delta^T D^T \leq \frac{1}{\eta} DD^T + \eta S^T S. \quad (12)$$

Lemma 3 ^[11] For matrices A_1, A_2, A_3 and Φ with appropriate dimensions and scalar φ , the following inequality holds,

$$A_1 + A_3^T A_2^T + A_2 A_3 < 0,$$

if the following conditions satisfied:

$$\begin{bmatrix} A_1 & \varphi A_2 + A_3^T \Phi^T \\ * & -\varphi \Phi - \varphi \Phi^T \end{bmatrix} < 0. \quad (13)$$

The goal of this paper is to construct an observer-based controller such that the system (8) is H_∞ FTB.

3. Main Results

In this part, sufficient conditions for FTB and H_∞ FTB of the system (8) via observer-based controller are devel-

oped.

3.1 Finite-time Boundedness

For expression convenience, we denote,

$$\theta_1 = \rho \varepsilon_1 + \beta \varepsilon_2, \theta_2 = -\frac{1}{2} \varepsilon_1 I + \frac{1}{2} \alpha \varepsilon_2 I, \quad \theta_3 = \rho \varepsilon_3 + \beta \varepsilon_4,$$

$$\theta_4 = -\frac{1}{2} \varepsilon_3 I + \frac{1}{2} \alpha \varepsilon_4 I, \quad \bar{P} = \begin{bmatrix} P & 0 \\ 0 & P \end{bmatrix}, \quad \bar{R} = \begin{bmatrix} R & 0 \\ 0 & R \end{bmatrix},$$

$$\lambda_1 = \lambda_{\max}(\bar{R}^{-\frac{1}{2}} \bar{P} \bar{R}^{-\frac{1}{2}}), \lambda_2 = \lambda_{\min}(\bar{R}^{-\frac{1}{2}} \bar{P} \bar{R}^{-\frac{1}{2}}), \lambda_3 = \lambda_{\max}(Q).$$

Theorem 1 Under Assumptions 1 and 2, system (8) is FTB with respect to (c_1, c_2, \bar{R}, N) , if there exist a known scalar φ , scalars $\mu \geq 1$, $\varepsilon_1 > 0, \varepsilon_2 > 0, \varepsilon_3 > 0, \varepsilon_4 > 0$, η_1, η_2 , symmetric matrices $P > 0, Q > 0$, and matrices Y, V, Φ , such that the following inequalities hold:

$$(1 + \mu)^N (\lambda_1 c_1 + \lambda_3 d^2) < c_2 \lambda_2, \quad (14)$$

$$\begin{bmatrix} \Theta_{11} & 0 & \Theta_{13} & 0 & 0 & \Theta_{16} & 0 & \Theta_{18} & 0 & 0 \\ * & \Theta_{22} & 0 & \Theta_{24} & 0 & \Theta_{26} & \Theta_{27} & \Theta_{28} & 0 & 0 \\ * & * & \Theta_{33} & 0 & 0 & P & 0 & 0 & 0 & 0 \\ * & * & * & \Theta_{44} & 0 & 0 & P & 0 & 0 & 0 \\ * & * & * & * & \Theta_{55} & P & P & 0 & 0 & 0 \\ * & * & * & * & * & \Theta_{66} & 0 & \Theta_{68} & \Theta_{69} & 0 \\ * & * & * & * & * & * & \Theta_{77} & 0 & \Theta_{79} & \Theta_{710} \\ * & * & * & * & * & * & * & \Theta_{88} & 0 & 0 \\ * & * & * & * & * & * & * & * & \Theta_{99} & 0 \\ * & * & * & * & * & * & * & * & * & \Theta_{1010} \end{bmatrix} < 0, \quad (15)$$

where

$$\begin{aligned} \Theta_{11} &= -(1 + \mu)P + \theta_1 I + \eta_1 N_1^T N_1 + \eta_2 N_2^T N_2, \\ \Theta_{13} &= \theta_2 I, \quad \Theta_{16} = A^T P - V^T B^T, \quad \Theta_{18} = -V^T, \\ \Theta_{22} &= \theta_3 I - (1 + \mu)P, \quad \Theta_{24} = \theta_4 I, \quad \Theta_{26} = V^T B^T, \\ \Theta_{27} &= A^T P - C^T Y^T, \quad \Theta_{28} = V^T, \quad \Theta_{33} = -\varepsilon_2 I, \\ \Theta_{44} &= -\varepsilon_4 I, \quad \Theta_{55} = -Q, \quad \Theta_{66} = -P, \\ \Theta_{68} &= \varphi(PB - B\Phi), \quad \Theta_{69} = PM_1, \quad \Theta_{77} = -P, \\ \Theta_{79} &= PM_2, \quad \Theta_{710} = -YM_2, \quad \Theta_{88} = -\varphi\Phi - \varphi\Phi^T, \\ \Theta_{99} &= -\eta_1 I, \quad \Theta_{1010} = -\eta_2 I. \end{aligned} \quad (16)$$

Furthermore, the controller gain is given by $K = \Phi^{-1}V$ and observer gain is $L = P^{-1}Y$.

Proof We first prove that the system (8) is FTB. So, we define the Lyapunov functional candidate as:

$$V_k = x_k^T P x_k + e_k^T P e_k, \quad P > 0. \quad (17)$$

Then, we have

$$\begin{aligned}
 & \Delta V_k - \mu V_k - w_k^T Q w_k \\
 = & x_{k+1}^T P x_{k+1} + e_{k+1}^T P e_{k+1} - (1+\mu) e_k^T P e_k - (1+\mu) x_k^T P x_k \\
 & - w_k^T Q w_k \\
 = & [(A+\Delta A - BK)x_k + BK e_k + g(x_k) + w_k]^T \\
 & \times P [(A+\Delta A - BK)x_k + BK e_k + g(x_k) + w_k] \\
 & + [(A-LC)e_k + (\Delta A - L\Delta C)x_k + \tilde{g}(x_k, \hat{x}_k) + w_k]^T \\
 & \times P [(A-LC)e_k + (\Delta A - L\Delta C)x_k + \tilde{g}(x_k, \hat{x}_k) + w_k] \\
 & - (1+\mu) e_k^T P e_k - (1+\mu) x_k^T P x_k - w_k^T Q w_k,
 \end{aligned} \tag{18}$$

From (18), we get that

$$\Delta V_k - \mu V_k - w_k^T Q w_k = \zeta_k^T \Pi \zeta_k, \tag{19}$$

where

$$\zeta_k = \begin{bmatrix} x_k^T & e_k^T & g^T(x_k) & \tilde{g}^T(x_k, \hat{x}_k) & w_k^T \end{bmatrix}^T,$$

$$\Pi = \begin{bmatrix} \Pi_{11} & \Pi_{12} & \Pi_{13} & \Pi_{14} & \Pi_{15} \\ * & \Pi_{22} & \Pi_{23} & \Pi_{24} & \Pi_{25} \\ * & * & P & 0 & P \\ * & * & * & P & P \\ * & * & * & * & 2P - Q \end{bmatrix},$$

$$\begin{aligned}
 \Pi_{11} &= (A + \Delta A - BK)^T P (A + \Delta A - BK) \\
 &+ (\Delta A - L\Delta C)^T P (\Delta A - L\Delta C) - (1 + \mu)P, \\
 \Pi_{12} &= (A + \Delta A - BK)^T P BK + (\Delta A - L\Delta C)^T \times \\
 &P (A - LC), \\
 \Pi_{13} &= (A + \Delta A - BK)^T P, \quad \Pi_{14} = (\Delta A - L\Delta C)^T P, \\
 \Pi_{15} &= (A + \Delta A - BK)^T P + (\Delta A - L\Delta C)^T P, \\
 \Pi_{22} &= (BK)^T P BK + (A - LC)^T P (A - LC) \\
 &- (1 + \mu)P, \\
 \Pi_{23} &= (BK)^T P, \quad \Pi_{24} = (A - LC)^T P, \\
 \Pi_{25} &= (BK)^T P + (A - LC)^T P.
 \end{aligned}$$

From (5) and (6), it follows that

$$\varepsilon_1 \rho x_k^T x_k - \frac{1}{2} \varepsilon_1 g^T(x_k) x_k - \frac{1}{2} \varepsilon_1 x_k^T g(x_k) \geq 0, \tag{20a}$$

$$\begin{aligned}
 & \varepsilon_2 \beta x_k^T x_k + \frac{1}{2} \varepsilon_2 \alpha x_k^T g(x_k) + \frac{1}{2} \varepsilon_2 \alpha g^T(x_k) x_k \\
 & - \varepsilon_2 g^T(x_k) g(x_k) \geq 0,
 \end{aligned} \tag{20b}$$

$$-\varepsilon_3 \rho e_k^T e_k - \frac{1}{2} \varepsilon_3 \tilde{g}^T(x_k, \hat{x}_k) e_k - \frac{1}{2} \varepsilon_3 e_k^T \tilde{g}(x_k, \hat{x}_k) \geq 0, \tag{20c}$$

$$\begin{aligned}
 & \varepsilon_4 \beta e_k^T e_k + \frac{1}{2} \varepsilon_4 \alpha e_k^T \tilde{g}(x_k, \hat{x}_k) + \frac{1}{2} \alpha \varepsilon_4 \tilde{g}^T(x_k, \hat{x}_k) e_k \\
 & - \varepsilon_4 \tilde{g}^T(x_k, \hat{x}_k) \tilde{g}(x_k, \hat{x}_k) \geq 0,
 \end{aligned} \tag{20d}$$

where $\varepsilon_1, \varepsilon_2, \varepsilon_3$ and ε_4 are arbitrary strictly positive scalars.

From the inequality (20a-20d), we can obtain that

$$\zeta_k^T \begin{bmatrix} \theta_1 I & 0 & \theta_2 I & 0 & 0 \\ * & \theta_3 I & 0 & \theta_4 I & 0 \\ * & * & -\varepsilon_2 I & 0 & 0 \\ * & * & * & -\varepsilon_4 I & 0 \\ * & * & * & * & 0 \end{bmatrix} \zeta_k \geq 0. \tag{21}$$

Then, the following inequality is obtained by adding the left hand side of (21) to (19)

$$\Delta V_k - \mu V_k - w_k^T Q w_k \leq \zeta_k^T \Omega \zeta_k,$$

where

$$\Omega = \begin{bmatrix} \Omega_{11} & \Pi_{12} & \Omega_{13} & \Pi_{14} & \Pi_{15} \\ * & \Omega_{22} & \Pi_{23} & \Omega_{24} & \Pi_{25} \\ * & * & \Omega_{33} & \Pi_{34} & P \\ * & * & * & \Omega_{44} & P \\ * & * & * & * & 2P - Q \end{bmatrix}, \tag{22}$$

$$\begin{aligned}
 \Omega_{11} &= \Pi_{11} + \theta_1 I, \quad \Omega_{13} = \Pi_{13} + \theta_2 I, \\
 \Omega_{22} &= \Pi_{22} + \theta_3 I, \quad \Omega_{24} = \Pi_{24} + \theta_4 I, \\
 \Omega_{33} &= P - \varepsilon_2 I, \quad \Omega_{44} = P - \varepsilon_4 I.
 \end{aligned}$$

By using Lemma 1, it is obvious that $\Omega < 0$ is equivalent to

$$\Xi = \begin{bmatrix} \Xi_{11} & 0 & \theta_2 I & 0 & 0 & \Xi_{16} & \Xi_{17} \\ * & \Xi_{22} & 0 & \theta_4 I & 0 & \Xi_{26} & \Xi_{27} \\ * & * & \Xi_{33} & 0 & 0 & P & 0 \\ * & * & * & \Xi_{44} & 0 & 0 & P \\ * & * & * & * & -Q & P & P \\ * & * & * & * & * & -P & 0 \\ * & * & * & * & * & * & -P \end{bmatrix} < 0, \tag{23}$$

where

$$\begin{aligned}
 \Xi_{11} &= -(1 + \mu)P + \theta_1 I, \quad \Xi_{16} = (A + \Delta A - BK)^T P, \\
 \Xi_{17} &= (\Delta A - L\Delta C)^T P, \quad \Xi_{22} = \theta_3 I - (1 + \mu)P, \\
 \Xi_{26} &= (BK)^T P, \quad \Xi_{27} = (A - LC)^T P, \\
 \Xi_{33} &= -\varepsilon_2 I, \quad \Xi_{44} = -\varepsilon_4 I.
 \end{aligned}$$

By segregating the matrix (23) for known and uncertain parts, yield

$$\begin{aligned} \Xi = & \begin{bmatrix} \Xi_{11} & 0 & \theta_2 I & 0 & 0 & (A-BK)^T P & 0 \\ * & \Xi_{22} & 0 & \theta_4 I & 0 & (BK)^T P & (A-LC)^T P \\ * & * & \Xi_{33} & 0 & 0 & P & 0 \\ * & * & * & \Xi_{44} & 0 & 0 & P \\ * & * & * & * & -Q & P & P \\ * & * & * & * & * & -P & 0 \\ * & * & * & * & * & * & -P \end{bmatrix} \\ + & \begin{bmatrix} 0 & 0 & 0 & 0 & 0 & \Delta A^T P & (\Delta A-L\Delta C)^T P \\ * & 0 & 0 & 0 & 0 & 0 & 0 \\ * & * & 0 & 0 & 0 & 0 & 0 \\ * & * & * & 0 & 0 & 0 & 0 \\ * & * & * & * & 0 & 0 & 0 \\ * & * & * & * & * & 0 & 0 \\ * & * & * & * & * & * & 0 \end{bmatrix} < 0. \end{aligned} \quad (24)$$

Then, inequality (24) can be rewritten as:

$$\Xi = \Xi_1 + \Xi_2 + \Xi_3 < 0, \quad (25)$$

where

$$\Xi_1 = \begin{bmatrix} \Xi_{11} & 0 & \theta_2 I & 0 & 0 & A^T P & 0 \\ * & \Xi_{22} & 0 & \theta_4 I & 0 & 0 & (A-LC)^T P \\ * & * & \Xi_{33} & 0 & 0 & P & 0 \\ * & * & * & \Xi_{44} & 0 & 0 & P \\ * & * & * & * & -Q & P & P \\ * & * & * & * & * & -P & 0 \\ * & * & * & * & * & * & -P \end{bmatrix},$$

$$\Xi_2 = \begin{bmatrix} 0 & 0 & 0 & 0 & 0 & \Delta A^T P & (\Delta A-L\Delta C)^T P \\ * & 0 & 0 & 0 & 0 & 0 & 0 \\ * & * & 0 & 0 & 0 & 0 & 0 \\ * & * & * & 0 & 0 & 0 & 0 \\ * & * & * & * & 0 & 0 & 0 \\ * & * & * & * & * & 0 & 0 \\ * & * & * & * & * & * & 0 \end{bmatrix},$$

$$\Xi_3 = \begin{bmatrix} 0 & 0 & 0 & 0 & 0 & -(BK)^T P & 0 \\ * & 0 & 0 & 0 & 0 & (BK)^T P & 0 \\ * & * & 0 & 0 & 0 & 0 & 0 \\ * & * & * & 0 & 0 & 0 & 0 \\ * & * & * & * & 0 & 0 & 0 \\ * & * & * & * & * & 0 & 0 \\ * & * & * & * & * & * & 0 \end{bmatrix}.$$

In order to deal with the nonlinear term $K^T B^T P$ and $-K^T B^T P$ in (25), a non-singular matrix Φ is introduced and defined $K = \Phi^{-1}V$, it is obvious that

$$P^T BK = (P^T B - B\Phi)\Phi^{-1}V + BV. \quad (26)$$

From (26), we can deduce

$$\begin{aligned} \Xi = & \underbrace{\tilde{\Xi}_1}_{\mathcal{A}_1} + \underbrace{\tilde{\Xi}_2}_{\mathcal{A}_2} \\ + He & \begin{bmatrix} 0 \\ 0 \\ 0 \\ 0 \\ 0 \\ 0 \\ PB-B\Phi \\ 0 \end{bmatrix} \underbrace{\Phi^{-1}[-V \ V \ 0 \ 0 \ 0 \ 0 \ 0 \ 0]}_{\mathcal{A}_3} \end{bmatrix} < 0, \quad (27)$$

< 0,

where

$$\tilde{\Xi}_1 = \begin{bmatrix} \tilde{\Xi}_{11} & 0 & \theta_2 I & 0 & 0 & \tilde{\Xi}_{16} & 0 \\ * & \tilde{\Xi}_{22} & 0 & \theta_4 I & 0 & \tilde{\Xi}_{26} & \tilde{\Xi}_{27} \\ * & * & \tilde{\Xi}_{33} & 0 & 0 & P & 0 \\ * & * & * & \tilde{\Xi}_{44} & 0 & 0 & P \\ * & * & * & * & -Q & P & P \\ * & * & * & * & * & -P & 0 \\ * & * & * & * & * & * & -P \end{bmatrix}$$

$$\tilde{\Xi}_{16} = A^T P - V^T B^T,$$

$$\tilde{\Xi}_{26} = V^T B^T,$$

$$\tilde{\Xi}_{27} = (A-LC)^T P,$$

$$Y = PL.$$

By Lemma 3, we can obtain that (27) holds if

$$\tilde{\Xi} = \begin{bmatrix} \tilde{\Xi}_1 + \tilde{\Xi}_2 & \hat{\Xi} \\ * & -\varphi\Phi - \varphi\Phi^T \end{bmatrix} < 0, \quad (28)$$

where

$$\hat{\Xi} = \varphi\mathcal{A}_2 + \mathcal{A}_3^T \Phi^T = \varphi \begin{bmatrix} 0 \\ 0 \\ 0 \\ 0 \\ 0 \\ 0 \\ PB-B\Phi \\ 0 \end{bmatrix} + \begin{bmatrix} -V^T \\ V^T \\ 0 \\ 0 \\ 0 \\ 0 \\ 0 \\ 0 \end{bmatrix} \Phi^{-T} \Phi^T = \begin{bmatrix} -V^T \\ V^T \\ 0 \\ 0 \\ 0 \\ 0 \\ \varphi(PB-B\Phi) \\ 0 \end{bmatrix}.$$

Now, by using Equation (3), (28) can be rewritten as

$$\begin{aligned} \tilde{\Xi} &= \begin{bmatrix} \tilde{\Xi}_1 & \hat{\Xi} \\ * & -\varphi\Phi - \varphi\Phi^T \end{bmatrix} + S_1\Delta_1(k)D_1 \\ &+ D_1^T\Delta_1^T(k)S_1^T + S_2\Delta_2(k)D_2 + D_2^T\Delta_2^T(k)S_2^T < 0, \end{aligned} \quad (29)$$

where

$$\begin{aligned} D_1 &= [N_1 \ 0 \ 0 \ 0 \ 0 \ 0 \ 0 \ 0], \\ S_1^T &= [0 \ 0 \ 0 \ 0 \ 0 \ M_1^T P \ M_2^T P \ 0], \\ D_2 &= [N_2 \ 0 \ 0 \ 0 \ 0 \ 0 \ 0 \ 0], \\ S_2^T &= [0 \ 0 \ 0 \ 0 \ 0 \ 0 \ -M_2^T Y^T \ 0]. \end{aligned}$$

Now, using Lemma 2, (29) holds if

$$\begin{aligned} &\begin{bmatrix} \tilde{\Xi}_1 & \hat{\Xi} \\ * & -\varphi\Phi - \varphi\Phi^T \end{bmatrix} + \eta_1 D_1 D_1^T \\ &+ \eta_1^{-1} S_1^T S_1 + \eta_2 D_2 D_2^T + \eta_2^{-1} S_2^T S_2 < 0, \end{aligned} \quad (30)$$

for any $\eta_1 > 0, \eta_2 > 0$.

By using Lemma 1, (15) imply (30) holds. So, we have that $\Pi < 0$. Then

$$\Delta V_k - \mu V_k - w_k^T Q w_k < 0, \quad (31)$$

which implies that

$$V_{k+1} < (1 + \mu)V_k + w_k^T Q w_k. \quad (32)$$

From (32), we get that

$$\begin{aligned} V_k &< (1 + \mu)^k V_0 + \sum_{i=0}^{k-1} (1 + \mu)^{k-i-1} w_i^T Q w_i \\ &\leq (1 + \mu)^N V_0 + (1 + \mu)^{k-1} \lambda_{\max}(Q) d^2 \\ &\leq (1 + \mu)^N (V_0 + \lambda_3 d^2), \end{aligned} \quad (33)$$

From (17), we have

$$\begin{aligned} V_0 &= x_0^T P x_0 + e_0^T P e_0 \\ &= \bar{x}_0^T \bar{R}^{\frac{1}{2}} \bar{R}^{-\frac{1}{2}} \bar{P} \bar{R}^{-\frac{1}{2}} \bar{R}^{\frac{1}{2}} \bar{x}_0 \\ &\leq \lambda_{\max}(\bar{R}^{-\frac{1}{2}} \bar{P} \bar{R}^{-\frac{1}{2}}) \bar{x}_0^T \bar{R} \bar{x}_0 \\ &\leq \lambda_1 c_1, \end{aligned} \quad (34)$$

$$\begin{aligned} V_k &= \bar{x}_k^T \bar{P} \bar{x}_k \\ &= \bar{x}_k^T \bar{R}^{\frac{1}{2}} \bar{R}^{-\frac{1}{2}} \bar{P} \bar{R}^{-\frac{1}{2}} \bar{R}^{\frac{1}{2}} \bar{x}_k \\ &\geq \lambda_{\min}(\bar{R}^{-\frac{1}{2}} \bar{P} \bar{R}^{-\frac{1}{2}}) \bar{x}_k^T \bar{R} \bar{x}_k \\ &= \lambda_2 \bar{x}_k^T \bar{R} \bar{x}_k, \end{aligned} \quad (35)$$

So, from (33)-(35), one get

$$\begin{aligned} \lambda_2 \bar{x}_k^T \bar{R} \bar{x}_k &< (1 + \mu)^N (V_0 + \lambda_3 d^2) \\ &< (1 + \mu)^N (\lambda_1 c_1 + \lambda_3 d^2), \end{aligned} \quad (36)$$

Using (14), we get that

$$\bar{x}_k^T \bar{R} \bar{x}_k < c_2.$$

According to Definition 1, the system (8) is FTB. This completes the proof.

Remark 2 For a given μ , the inequality (15) is linear matrices inequality which can be solved by MATLAB LMIs Toolbox to obtain matrices $P > 0, Q > 0$, and matrices Y, V, Φ .

3.2 H_∞ Finite-time Boundedness

Theorem 2 Given a scalar $\gamma > 0$. Under Assumptions 1 and 2, the closed-loop system (8) is H_∞ FTB with respect to $(c_1, c_2, \bar{R}, N, \gamma)$, if there exist a known scalar φ , scalars $\mu \geq 1, \varepsilon_1 > 0, \varepsilon_2 > 0, \varepsilon_3 > 0, \varepsilon_4 > 0, \eta_1, \eta_2$, symmetric matrices $P > 0, Q > 0$, and matrices Y, V, Φ such that the following inequalities hold:

$$(1 + \mu)^N (\lambda_1 c_1 + \lambda_3 d^2) < c_2 \lambda_2, \quad (37)$$

$$\begin{bmatrix} \Theta_1 & \Theta_2 \\ * & \Theta_3 \end{bmatrix} < 0, \quad (38)$$

where

$$\Theta_1 = \begin{bmatrix} \tilde{\Theta}_{11} & 0 & \Theta_{13} & 0 & E^T F \\ * & \Theta_{22} & 0 & \Theta_{24} & 0 \\ * & * & \Theta_{33} & 0 & 0 \\ * & * & * & \Theta_{44} & 0 \\ * & * & * & * & \tilde{\Theta}_{55} \end{bmatrix},$$

$$\Theta_2 = \begin{bmatrix} \Theta_{16} & 0 & \Theta_{18} & 0 & 0 \\ \Theta_{26} & \Theta_{27} & \Theta_{28} & 0 & 0 \\ P & 0 & 0 & 0 & 0 \\ 0 & P & 0 & 0 & 0 \\ 0 & 0 & 0 & 0 & 0 \end{bmatrix},$$

$$\Theta_3 = \begin{bmatrix} \Theta_{66} & 0 & \Theta_{68} & \Theta_{69} & 0 \\ * & \Theta_{77} & 0 & \Theta_{79} & \Theta_{7,10} \\ * & * & \Theta_{88} & 0 & 0 \\ * & * & * & \Theta_{99} & 0 \\ * & * & * & * & \Theta_{10,10} \end{bmatrix},$$

$$\tilde{\Theta}_{11} = \Theta_{11} + E^T E, \quad \tilde{\Theta}_{55} = -\frac{\gamma^2}{(1 + \mu)^N} I + F^T F,$$

and other parameters are given in (16). Furthermore, the controller gain is given by $K = \Phi^{-1} V$ and the observer gain is $L = P^{-1} Y$.

Proof. We show that for any $w_k \neq 0$, under the zero-initial condition the output z_k satisfies

$$\sum_{k=0}^N z_k^T z_k < \gamma^2 \sum_{k=0}^N w_k^T w_k.$$

Choose the same Lyapunov function as (17) and define

$$J_k = \Delta V_k - \mu V_k + z_k^T z_k - w_k^T Q w_k. \quad (39)$$

Let

$$Q = \frac{\gamma^2}{(1+\mu)^N} I.$$

Then from (38), we have

$$J_k < 0. \tag{40}$$

From (40), it is obvious that

$$V_k < \sum_{i=0}^{k-1} (1+\mu)^{k-i-1} [w_i^T Q w_i - z_i^T z_i] + (1+\mu)^k V_0.$$

Under zero-initial conditions, $V_k \geq 0$ and $V_0 = 0$. Therefore, we have

$$0 < \sum_{i=0}^{k-1} (1+\mu)^{k-i-1} [w_i^T Q w_i - z_i^T z_i].$$

It follows that

$$\sum_{i=0}^{k-1} z_i^T z_i < \sum_{i=0}^{k-1} (1+\mu)^N \frac{\gamma^2}{(1+\mu)^N} w_i^T w_i.$$

It is deduced that

$$\sum_{i=0}^N z_i^T z_i < \gamma^2 \sum_{i=0}^N w_i^T w_i. \tag{41}$$

From (40), it is obvious that (31) holds. From Theorem 1, we get that the system (8) is FTB.

According to Definition 2, the system (8) is H_∞ finite-time boundedness. The proof is completed.

Remark 3 For a given μ , the inequality (38) is a linear matrix inequality which can be solved by MATLAB LMIs Toolbox to obtain matrices $P > 0, Q > 0$, and matrices Y, V, Φ .

Remark 4 The system (8) considered in Theorem 2 has parameter uncertainty. However, systems that are often encountered in practical have no parameter uncertainty, so it is also necessary to study H_∞ finite time boundedness for the system (8) with no parameter uncertainty. The following corollary gives a sufficient condition of H_∞ finite time boundedness for (8) with $\Delta A(k) = 0, \Delta C(k) = 0$.

Corollary 1 Given a scalar $\gamma > 0$. Under Assumptions 1 and 2, the closed-loop system (8) with $\Delta A(k) = 0, \Delta C(k) = 0$ is H_∞ finite-time boundedness with respect to $(c_1, c_2, \bar{R}, N, \gamma)$, if there exist a known scalar φ , scalars $\mu \geq 1, \varepsilon_1 > 0, \varepsilon_2 > 0, \varepsilon_3 > 0, \varepsilon_4 > 0$, symmetric matrices $P > 0$, and matrices Y, V, Φ , such that the following inequalities hold:

$$(1+\mu)^N (\lambda_1 c_1 + \lambda_3 d^2) < c_2 \lambda_2,$$

$$\begin{bmatrix} \hat{\Theta}_{11} & 0 & \Theta_{13} & 0 & E^T F & \Theta_{16} & 0 & -V^T \\ * & \Theta_{22} & 0 & \Theta_{24} & 0 & \Theta_{26} & \Theta_{27} & V^T \\ * & * & \Theta_{33} & 0 & 0 & P & 0 & 0 \\ * & * & * & \Theta_{44} & 0 & 0 & P & 0 \\ * & * & * & * & \tilde{\Theta}_{55} & 0 & 0 & 0 \\ * & * & * & * & * & -P & 0 & \Theta_{68} \\ * & * & * & * & * & * & -P & 0 \\ * & * & * & * & * & * & * & \Theta_{88} \end{bmatrix} < 0,$$

where $\hat{\Theta}_{11} = -(1+\mu)P + \theta_1 I + E^T E$, and other parameters are given in (16). Furthermore, the controller gain is given by $K = \Phi^{-1} V$ and observer gain is $L = P^{-1} Y$.

Proof. The proof is similar to the proof of Theorem 2, omitted here.

Remark 5. Some new criteria of observer-based finite-time H_∞ control for discrete-time one-sided Lipschitz systems with uncertainties are given in Theorems 1 and 2. The main novelty of equation (26) is that the bilinear term $P^x B K$ can be eliminated by defining matrix variables Φ and V .

4. Numerical Example

In this section, a numerical example is given to show the application of the developed theory.

Example 1. Consider the nonlinear system (1) with the following parameters:

$$A = \begin{bmatrix} 0.1 & 0.01 \\ 0.02 & 0.1 \end{bmatrix}, B = \begin{bmatrix} 0.1 & 0.1 \\ 0.1 & 0.12 \end{bmatrix},$$

$$C = \begin{bmatrix} -0.3 & 0.1 \\ 0.3 & 0.1 \end{bmatrix}, E = \begin{bmatrix} 0.02 & 0.1 \\ 0.2 & 0.1 \end{bmatrix},$$

$$F = \begin{bmatrix} 0.01 & 0.2 \\ 0.2 & 0.01 \end{bmatrix},$$

$$g(x_k) = \begin{bmatrix} 0.02 \sin(x_k) \\ 0.02 \sin(x_k) \end{bmatrix},$$

$$w_k = \begin{bmatrix} e^{-0.2k} \sin(k) \\ e^{-0.2k} \sin(k) \end{bmatrix}, x_k = \begin{bmatrix} x_{1k} \\ x_{2k} \end{bmatrix}.$$

$$M_1 = \begin{bmatrix} 0.12 & 0.03 \\ 0.03 & 0.12 \end{bmatrix}, M_2 = \begin{bmatrix} 0.11 & 0.02 \\ 0.02 & 0.11 \end{bmatrix},$$

$$N_1 = \begin{bmatrix} 0.01 & 0.01 \\ 0.01 & 0.01 \end{bmatrix}, N_2 = \begin{bmatrix} 0.02 & 0.02 \\ 0.02 & 0.02 \end{bmatrix}.$$

Take $\varphi = 0.5, \eta_1 = \eta_2 = 2, c_1 = 0.2, \mu = 0.001, \gamma = 1, \rho = 0.01, \alpha = -0.3, \beta = -0.5, \varepsilon_1 = \varepsilon_2 = \varepsilon_3 = \varepsilon_4 = 1$.

By using the MATLAB LMI toolbox, solving (37) and (38) leads to feasible solutions as follows:

$$P = \begin{bmatrix} 0.2110 & 0.0051 \\ 0.0051 & 0.1978 \end{bmatrix}, V = \begin{bmatrix} -0.1363 & -0.0827 \\ -0.0827 & -0.1214 \end{bmatrix},$$

$$\Phi = \begin{bmatrix} 8.9821 & -5.3997 \\ -5.3997 & 7.8462 \end{bmatrix}, Y = \begin{bmatrix} 0.0633 & -0.3720 \\ -0.3720 & -0.4188 \end{bmatrix}.$$

The controller and observer gains are

$$K = \begin{bmatrix} -0.0367 & -0.0316 \\ -0.0358 & -0.0372 \end{bmatrix},$$

$$L = \begin{bmatrix} 0.3458 & -1.7128 \\ -1.8898 & -2.0734 \end{bmatrix}.$$

According to Theorem 2, system (8) is H_∞ finite-time boundedness with respect to $(0.2, 5.48, I_4, 40, 1)$. Figure 1 and Figure 2 show the state trajectories of x_k and \hat{x}_k .

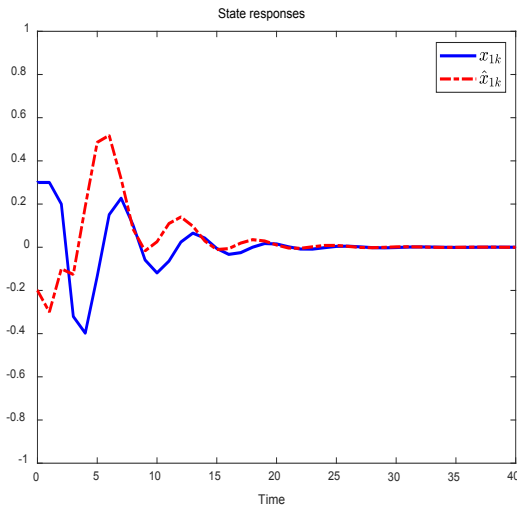


Figure 1. The trajectories of x_{1k} and \hat{x}_{1k} .

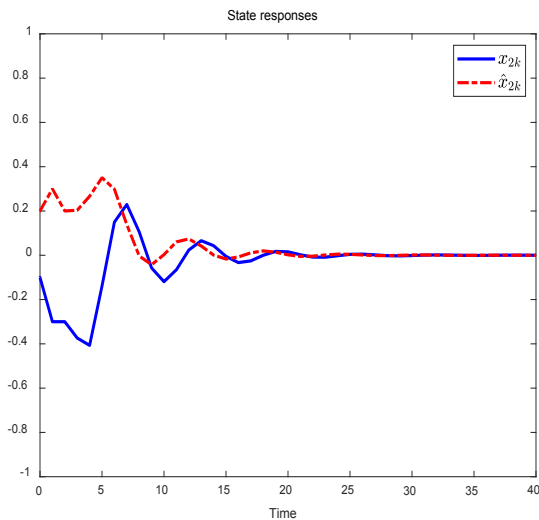


Figure 2. The trajectories of x_{2k} and \hat{x}_{2k} .

The trajectory of $\bar{x}_k^T \bar{R} \bar{x}_k$ is shown in Figure 3. It can be

seen from Figure 3 that when $k=1,2,\dots,40$, the value of $\bar{x}_k^T \bar{R} \bar{x}_k$ is less than c_2 .

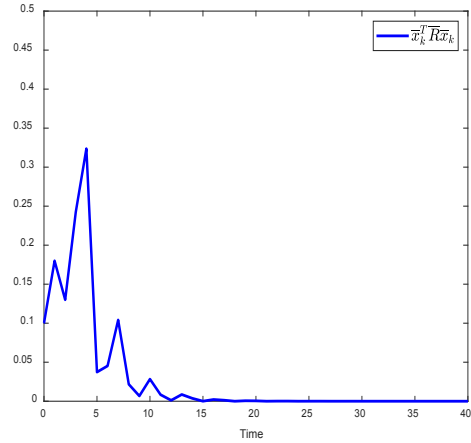


Figure 3. The trajectory of $\bar{x}_k^T \bar{R} \bar{x}_k$.

5. Conclusions

The paper discusses the observer-based finite-time H_∞ control problem for a class of one-sided Lipschitz nonlinear discrete-time system with parameter uncertainties and external disturbances. By using one-sided Lipschitz condition and inner-bounded condition, a new criterion is obtained to ensure the closed-loop system is H_∞ FTB. The observer and controller gains are designed. Finally, a numerical example is provided to demonstrate the applicability and reduced conservativeness of the presented results. Furthermore, this paper does not consider time-varying delay. Therefore, the problem of observer-based finite-time H_∞ control for nonlinear discrete-time systems with time-varying delay can be investigated in the future work.

Acknowledgments

This work was supported by the Natural Science Foundation of Tianjin under Grant No. 18JCYBJC88000.

Conflicts of Interest

The author declares that they have no conflicts of interest to report regarding the present study.

References

- [1] Dong, H.L., Wang, Z.D., Gao, H.D., 2010. Observer-based H_∞ control for systems with repeated scalar nonlinearities and multiple packet losses. International Journal of Robust and Nonlinear Control. 20(12), 1363-1378.
- [2] Wang, W., Ma, S.P., Zhang, C.H., 2013. Stability and static output feedback stabilization for a class of non-

- linear discrete-time singular switched systems. *International Journal of Control Automation and Systems*. 11(6), 1138-1148.
- [3] Wang, J.M., Ma, S.P., Zhang, C.H., 2017. Finite-time stabilization for nonlinear discrete-time singular Markov jump systems with piecewise-constant transition probabilities subject to average dwell time. *Journal of the Franklin Institute*. 354(5), 2102-2124.
- [4] Wang, J.M., Ma, S.P., Zhang, C.H., 2016. Stability analysis and stabilization for nonlinear continuous-time descriptor semi-Markov jump systems. *Applied Mathematics and Computation*. 279, 90-102.
- [5] Abbaszadeh, M., Marquez, H., 2010. Nonlinear observer design for one-sided Lipschitz systems. *American Control Conference*. pp. 5284-5289.
- [6] Du, Z.P., Yuan, W.R., Hu, S.L., 2019. Discrete-time event triggered H-infinity stabilization for networked cascade control systems with uncertain delay. *Journal of the Franklin Institute Engineering and Applied Mathematics*. 356(16), 9524-9544.
- [7] Song, Y., Fan, J., Fei, M.R., et al., 2008. Robust H_∞ control of discrete switched system with time delay. *Applied Mathematics and Computation*. 205(1), 159-169.
- [8] Wang, R., Wang, B., Liu, G.P., et al., 2010. H_∞ controller design for networked predictive control systems based on the average dwell-time approach. *IEEE Transactions on Circuits and Systems*. 579(4), 310-314.
- [9] Chen, H.F., Gao, J.F., Shi, T., et al., 2016. H_∞ control for networked control systems with time delay, data packet dropout and disorder. *Neurocomputing*. 179(29), 211-218.
- [10] Chang, X.H., Yang, G.H., 2014. New results on output feedback H_∞ control for linear discrete-time systems. *IEEE Transactions on Automatic Control*. 59(5), 1355-1359.
- [11] Chang, X.H., Zhang, L., Park, J.H., 2015. Robust static output feedback H_∞ control for uncertain fuzzy systems. *Fuzzy Sets and Systems*. 273(15), 87-104.
- [12] Miao, X.F., Xu, Y.Q., Yao, F.G., 2021. Observers design for a class of nonlinear stochastic discrete-time systems. *International Journal of Theoretical Physics*. 60(7), 26042612.
- [13] Badreddine, E., Hicham, E., Abdelaziz, H., et al., 2019. New approach to robust observer-based control of one-sided Lipschitz non-linear systems. *IET Control Theory and Applications*. 13(3), 333-342.
- [14] Dong, H.L., Wang, Z.D., Gao, H.J., 2010. Observer-based H_∞ control for systems with repeated scalar nonlinearities and multiple packet losses. *International Journal of Robust and Nonlinear Control*. 20, 1363-1378.
- [15] Wang, J.X., Wu, H.C., Ji, X.F., et al., 2020. Robust finite-time stabilization for uncertain discrete-time linear singular systems. *IEEE Access*. 8, 100645-100651.
- [16] Feng, T., Wu, B.W., Liu, L.L., et al., 2019. Finite time stability and stabilization of fractional-order switched singular continuous-time system. *Circuits Systems and Signal Processing*. 38(12), 5528-5548.
- [17] Zhang, T.L., Deng, F.Q., Zhang, W.H., 2019. Finite-time stability and stabilization of linear discrete time-varying stochastic systems. *Journal of the Franklin Institute Engineering and Applied Mathematics*. 356(3), 1247-1267.
- [18] Ban, J., Kwon, W., Won, S., et al., 2018. Robust H_∞ finite-time control for discrete-time polytopic uncertain switched linear systems. *Nonlinear Analysis-Hybrid Systems*. 29, 348-362.
- [19] Benallouch, M., Boutayeb, M., Zasadzinski, M., 2012. Observer design for one-sided Lipschitz discrete-time systems. *Systems and Control Letters*. 61(9), 879-886.

ARTICLE

Monitoring Heart Rate Variability Based on Self-powered ECG Sensor Tag

Nhat Minh Tran¹ Ngoc-Giao Pham² Thang Viet Tran^{3*}

1. Department of Telecommunication, Sai Gon University, Vietnam

2. Department of Computing Fundamentals, FPT University, Hanoi, Vietnam

3. Department of Science and Technology, Nguyen Tat Thanh University, Ho Chi Minh City, Vietnam

ARTICLE INFO

Article history

Received: 1 November 2022

Revised: 9 November 2022

Accepted: 14 November 2022

Published Online: 25 November 2022

Keywords:

Batteryless ECG sensor

Heart rate monitoring

UHF RFID

ABSTRACT

This paper proposes a batteryless sensing and computational device to collect and process electrocardiography (ECG) signals for monitoring heart rate variability (HRV). The proposed system comprises of a passive UHF radio frequency identification (RFID) tag, an extreme low power microcontroller, a low-power ECG circuit, and a radio frequency (RF) energy harvester. The microcontroller and ECG circuits consume less power of only $\sim 30 \mu\text{A}$ and $\sim 3 \text{ mA}$, respectively. Therefore, the proposed RF harvester operating at frequency band of 902 MHz \sim 928 MHz can sufficiently collect available energy from the RFID reader to supply power to the system within a maximum distance of $\sim 2 \text{ m}$. To extract R-peak of the ECG signal, a robust algorithm that consumes less time processing is also developed. The information of R-peaks is stored into an Electronic Product Code (EPC) Class 1st Generation 1st compliant ID of the tag and read by the reader. This reader is functioned to collected the R-peak data with sampling rate of 100ms; therefore, the user application can monitor fully range of HRV. The performance of the proposed system shows that this study can provide a good solution in paving the way to new classes of healthcare applications.

1. Introduction

Wearable wireless body devices are widely deployed in health monitoring system nowadays. However, most of the distributed body sensor nodes consume more power due to wireless data transmission power^[1-3]. To overcome the serious drawback in specific applications, in this work,

the UHF RFID technology that does not require power to communicate with base station is considered instead of conventional wireless methods such as the ZigBee, BlueTooth, and WiFi standards. In addition, a RF energy harvester was designed to collect RF energy that is come from RFID reader for supplying power to the ECG sensor module. Therefore, the proposed system can power inde-

*Corresponding Author:

Thang Viet Tran,

Department of Science and Technology, Nguyen Tat Thanh University, Ho Chi Minh City, Vietnam;

Email: tvthang@ntt.edu.vn

DOI: <https://doi.org/10.30564/jeis.v4i2.5225>

Copyright © 2022 by the author(s). Published by Bilingual Publishing Co. This is an open access article under the Creative Commons Attribution-NonCommercial 4.0 International (CC BY-NC 4.0) License. (<https://creativecommons.org/licenses/by-nc/4.0/>).

pendently in normal operation duration.

HRV is one of critical parameters to diagnose a number of medical conditions, including diabetes, sleep apnea, cardiovascular diseases, and mental stress^[4]. HRV measurements are basically extracted from original ECG signals that are collected by wearable devices. These wearable devices traditionally transmitted data to the host over Bluetooth, ZigBee, or WiFi links^[5]. However, some wearable sensors for measuring the biomedical signals showed that the power consumption of wireless standards consumes significant average power of 14.8 mW and 30.7 mW in Bluetooth low energy (BLE) and ZigBee, respectively^[6]. In actual cases, assisted battery-based wearable devices need to replace battery after dozens of operating hours due to high wireless transmission power. Therefore, a compact, long life, real-time HVR assessment device has to be designed to enable and expand HVR diagnostic applications in future.

Recently RFID has become the critical component in the design of various applications in industries and social life. Emerging RFID applications extend from tracking areas, cold chain management, and patient identification^[7], to battery-less sensing applications using RF energy harvester. A low-cost and battery-less smart sensor tag operating at high frequency (HF) can measure temperature and relative humidity within distance of 30 cm for monitoring the freshness of packaged vegetable. To monitor temperature and humidity in far distance of 27 m in outdoor environment, a long-range UHF RFID tag with assisted solar panel was developed. Moreover, RFID sensor tag can be used to collect physiological signals from human body. A wearable UHF RFID-based smart tag that does not require battery can monitor electroencephalogram (EEG) signal at the distances up to 0.8 m. The autonomous sensor tags that operate at UHF band can measure ECG signals for monitoring HR and HRV^[8]. The structure of our paper is organized as follows: Section 2 presents the related works; Section 3 introduces a system design; Section 3 gives an explanation of the proposed algorithm; Section 4 describes experimental results; and conclusions is shown in Section 5.

2. Related Works

2.1 UHF RFID System

Basically, the RFID systems consist of small low-cost, wireless battery-free devices, called tags, which use the radio signal from a specialized RFID reader for power and communication. When queried, each tag responds to a unique identification number by reflecting energy back

to the reader through backscatter modulation. Tags are often application-specific fixed-function devices that have a range of 10 cm ~ 50 cm for high frequency (HF) devices and 3 m ~ 10 m for UHF tags^[9,10]. The development of RFID technology has produced a robust physical layer capable of wirelessly powering and querying a tag. This core technology enables a new class of wireless battery-free devices with communication. This study just focuses on design of the UHF RFID-based sensor tag that operates at frequency of ~915 MHz.

2.1.1 Types of RFID Tags

Typically there are three types of RFID tags, namely, passive, semi-passive, and active tags^[11]. The operation of each is shown in Figure 1.

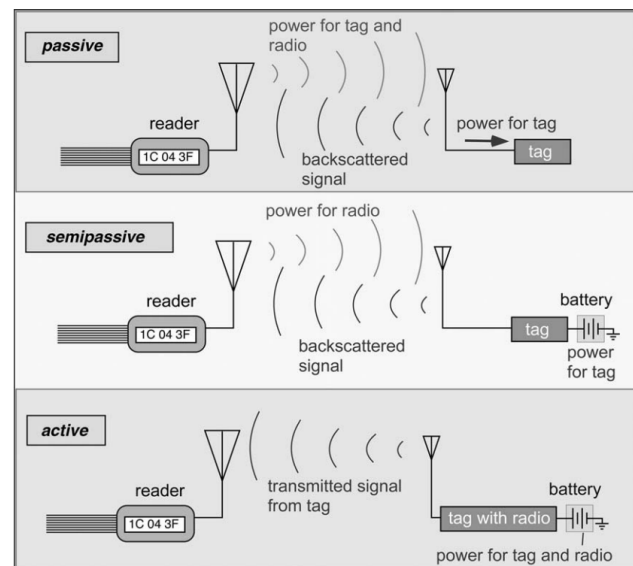


Figure 1. Configuration of three types of tags

Passive tag: This type of tags contains no power supply on board; therefore, they are very cheap and small. Passive tags absorb their energy when they enter an electromagnetic field (also called Near Field) created by RFID reader's antenna. The Near Field can be proximately calculated by the following equation: $r = \lambda / (2 * \pi)$, where λ is the wavelength. Due to the reason of no power supplied on board, the read range of passive tags is very short of several mm. Once a RFID reader has interrogated passive tags, and passive tags have absorbed enough energy, they use backscatter which is an RF technique to send their data back to RFID reader.

Semi-passive tag: The main difference is to require battery compared with passive tag. Batteries in semi-passive tags are only used to power the internal circuitry. The semi-passive tags still need to be presented inside the Near Filed in order to absorb power for data transmission

between RFID readers and themselves. The advantage of semi-passive tags is longer read ranges than passive tags because the energy they absorb from Near Field is fully used to transmit data only. Batteries in semi-active tags are used exactly the same as those in active tags; however, the energy will only be released to power the tags when the tags are being interrogated by RFID readers.

Active tag: Unlike passive tags, this type of tags comes with power supplied on board such as battery. Since they have their own power supply, they do not need to be powered by the Near Field of RFID readers' antennas. Therefore, passive tags have longer read range than passive tag. The drawbacks are that they are more expensive and bigger in size. Active tags send out signals which are encoded with their identifiers at regularly scheduled rate usually between 1 to 15 seconds.

2.1.2 UHF RFID Air Communication Protocol

There are two main air communication protocols that are involved in developing standards for UHF RFID technology, namely, EPCglobal (electronic product code) GEN2 (second-generation) and ISO (international standard organization) 1800-Part 6. In this study, the EPCglobal GEN2 is only considered due to the proposed application.

EPCglobal is a joint venture between Uniform Code Council (UCC) and EAN International. The organization carries the mission of the former Auto-ID (auto identification) Center at MIT (Massachusetts Institute of Technology). Its primary goal is to make the final EPC standard an official global standard. The EPC class types are summarized in Table 1 and an example of Electronic Product Code (EPC) structure is presented in Table 2 [12].

Table 1. EPC class types

| EPC class type | Feature | Tag type |
|----------------|--|---------------------------|
| Class 0 | Read only | Passive (64 bits only) |
| Class 1 | Write one/ Read many | Passive (96 bits minimum) |
| Class 2 | Read/Write | Passive (96 bits minimum) |
| Class 3 | Read/Write with battery power to enhance range | Semi-active |
| Class 4 | Read/Write active transmitter | Active |

2.1.3 Read Range Calculation

To calculate the reading range from the reader to the tag in frequency range of UHF band we can use the Friis equation. With the Friis equation, we can immediately draw the reversed link diagram for a directional antenna: the

received power is simply increased by antenna again [11]. The results are shown in Figure 2.

Table 2. EPC code structure

| Code | Representation |
|-----------|---|
| 01 | Version of EPC (8 bits header) |
| 115A1D7 | Manufacture Identifier; 28 bit (> 16 million possible manufactures) |
| 28A1E6 | Product Identifier; 24 bit (> 16 million possible products per manufacture) |
| 421CBA30A | Item Serial Number; 36 bit (> 68 billion possible unique items per product) |

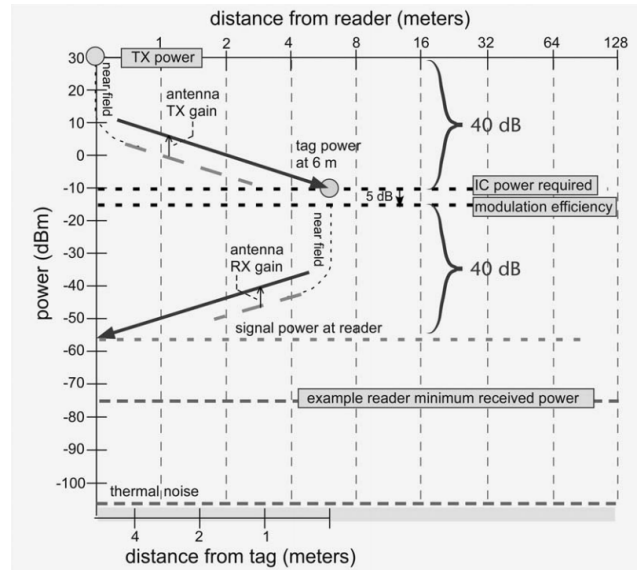


Figure 2. Forward and reverse link budgets for directional antenna

The received power is the same as in the isotropic case, even though the tag is twice as far away because the power at the tag is the same in both cases, and the received power is decreased by 6 dB due to the larger distance but increased by 6 dB due to the receiver antenna again. We can also construct a mathematical statement of the same relationships using the Friis equation by defining the gain of the tag antenna G_{tag} and a backscatter transmission loss $T_b (= 1/3 \text{ or } -5 \text{ dB})$. Then we have:

$$P_{TX,tag} = P_{TX,reader} G_{reader} G_{tag} \left(\frac{\lambda}{4\pi r} \right)^2 T_b \quad (1)$$

$$P_{RX,reader} = P_{TX,tag} G_{tag} G_{reader} \left(\frac{\lambda}{4\pi r} \right)^2 \quad (2)$$

$$P_{RX,reader} = P_{TX,reader} T_b G_{reader}^2 G_{tag}^2 \left(\frac{\lambda}{4\pi r} \right)^4 \quad (3)$$

In the most general case, the power received at the reader does as the inverse fourth power of (> the distance). It is also

proportional to the square of the antenna gains, so when reverse link power is important such as passive tag, the antenna gain plays a very large role in achievable read range. Real tag antennas have some gain, but it is typically modest (around 2 dB, since they are usually dipole-like), and since the application do not always control the exact orientation of the tag antenna and may not be able to guarantee that the main beam of the tag antenna is pointed at the reader, it is prudent to count on minimal gain from the tag antenna.

Using the Friis equation, we can also provide a couple of convenient range equations that can be useful for quick estimates. First, defining the minimum power, the tag requires as $P_{\min, \text{tag}}$, therefore the forward-link-limited range can be obtained:

$$R_{\text{forward}} = \left(\frac{\lambda}{4\pi} \right) \sqrt{\frac{P_{\text{TX}} G_{\text{reader}} G_{\text{tag}}}{P_{\min, \text{tag}}}} \quad (4)$$

and defining the minimum signal power for demodulation at the reader as $P_{\min, \text{rdr}}$, the reverse-link-limited range can be obtained:

$$R_{\text{reverse}} = \left(\frac{\lambda}{4} \right) \sqrt{\frac{P_{\text{TX}, \text{reader}} T_b G_{\text{reader}}^2 G_{\text{tag}}^2}{P_{\min, \text{rdr}}}} \quad (5)$$

2.2 Real-time ECG R-peak Detection Algorithm

Traditionally ECG waveforms are usually recorded in a clinical setting by medical professionals using twelve leads attached to the patient [13]. This work has developed a three-lead ECG device for use by person at home. The ECG signals recorded by human body with a three-lead suffer greatly from baseline wandering and high frequency noises, as compared to ECG signals recorded with twelve-leads in a clinical setting. Therefore, an accurate R-peak detection algorithm is an important step in ECG analysis. Various methods have been proposed in the past to detect R-peak under challenge conditions by using wavelet transform or Hilbert transform [14-16]. However, abovementioned methods consume more processing time and that suite to be applied in PC application or high-speed smart phones. In this study, we propose a new real-time R-peak detection algorithm for three-lead mobile ECG recordings. The proposed algorithm is simple to implement, computationally efficient, and does not require any signal pre-processing. This conceptual simplicity is a quality that distinguishes our approach from existing solutions. And therefore, the proposed algorithm consumes less processing time and can easily be applied into firmware for low-speed MCU based applications.

2.2.1 Characteristics of ECG Waveforms under Challenge Conditions

Recording ECG waveforms under motion artifacts and

respiration conditions causes the signals containing data losses, low and high frequency noises. Figure 3 shows an example of the ECG waveforms with data loss. Therefore the R-R interval in case of data loss is difficult to release by conventional R-peak detection method. Basically, the ECG comprises four different waves, namely, Q-wave, R-wave, S-wave, and T-wave; among them, R-wave and T-wave have higher amplitude compared to others. Most of cases, R-wave amplitude is bigger than T-wave. However, in specific case, as shown in Figure 4, the T-wave amplitude can compare with R-wave due to motion artifacts or respiration conditions. In this case, the R-peak detection method is easy to makemistakes. Therefore, the proposed algorithm focuses on considering those errors to overcome.

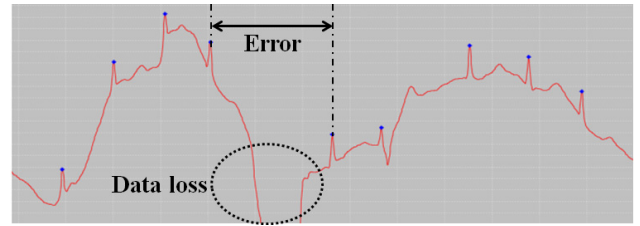


Figure 3. ECG waveforms with data loss

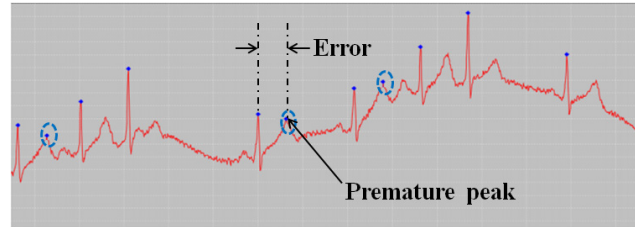


Figure 4. ECG waveforms under motion artifacts or respiration conditions

2.2.2 Algorithm

The proposed algorithm is a modified algorithm that was studied in previous work for real-time peak detection of PPG signals [17]. Figure 5 shows the operation of the proposed R-peak detection method.

In this method, a threshold distance that was described in Equation (6) is used to detect R-peak as following:

The reference distance is an adaptive value, d_{adt} , given by Equation (1).

In Equation (1), K is a dynamic value that depends on the peak-peak amplitude (VP-P) of the AC component in the PPG signal; n is the number of samples from the last local extreme point to the current point; hc is the current heart rate; fs is the sampling frequency. With each new detected R-peak, If EP_{pos} , which is the distance from the previous R-peak point to the current one, is lower than RP , the peak is considered to

be a fake point and is removed as shown in Figure 6. Therefore, the problem in Figure 4 will be solved. In the proposed method, refractory period (RP) that enables us to determine the premature peaks and d_{th} are empirically chosen as 55% of the previous R-R value and 5% of the previous extreme point amplitude, respectively.

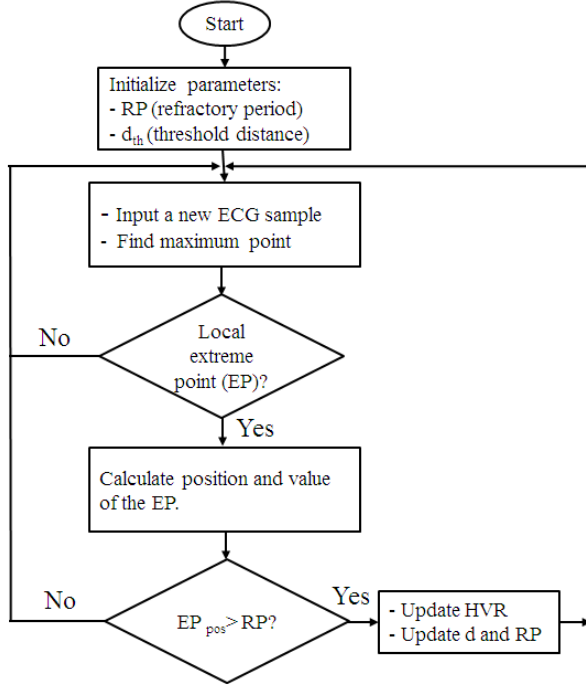


Figure 5. Proposed real-time R-peak detection method

$$d_{adt} = K * \left(1 - \frac{n * h_c}{30 * f_s}\right) \quad (6)$$

The proposed method can accurately detect R-peak of ECG waveforms under challenge conditions and eliminate error peak like premature peaks. However, some error peaks that come from data loss problems as shown in Figure 3 cannot be moved by the proposed method. Therefore, the random error detection method is used to eliminate those error peaks.

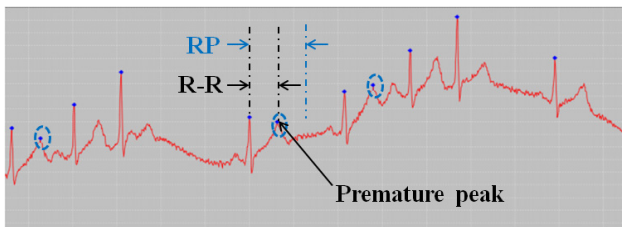


Figure 6. Comparison between R-R and RP for eliminating error peaks

3. System Design & Implementation

The integration of sensing capability into UHF RFID

tags has recently generated a lot of interest among the RFID community^[10,18,19]. In any sensor enabled RFID system data collection is done continuously. Data collection in this context can refer to the computation of statistical means and moments, as well as other cumulative quantities that summarize the data obtained by the system. One of important application areas is healthcare where sensor enabled RFID tags are used in hospitals, clinics, and at home to provide various healthcare services by collecting different environmental and physiological data^[20]. This work also focused on design a health-monitoring system based on RFID technology applying in home healthcare services.

Figure 7 shows the block diagram of the proposed system, including a UHF RFID tag, a MCU, an ECG module, a voltage monitor module, and RF energy harvester. The tag that does not require battery can wirelessly communicate with RFID reader. In this work, the proposed system can be powered by energy from the RF harvester that operates at the frequency of ~915 MHz to collect available RF energy from the reader. However, received RF energy is not always sufficient to supply to the system. Therefore a voltage monitor is designed to manage the power. The proposed ECG sensor tag can collect ECG signal, then the received data are processed and transmitted to the host over the reader as shown in Figure 8.

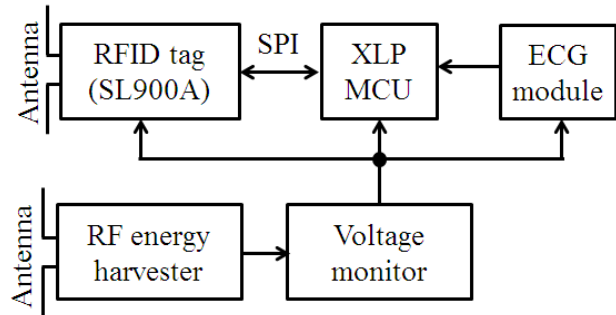


Figure 7. Block diagram of the proposed ECG sensor tag

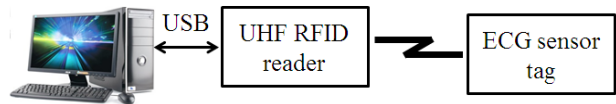


Figure 8. Architecture of the proposed UHF RFID system

3.1 RFID Tag

The RFID tag is built around the SL900A (AMS Co., Australia) that is an EPC global class 1 and class 3 compliant tag chip. Figure 9 shows the block diagram of the tag chip^[21].

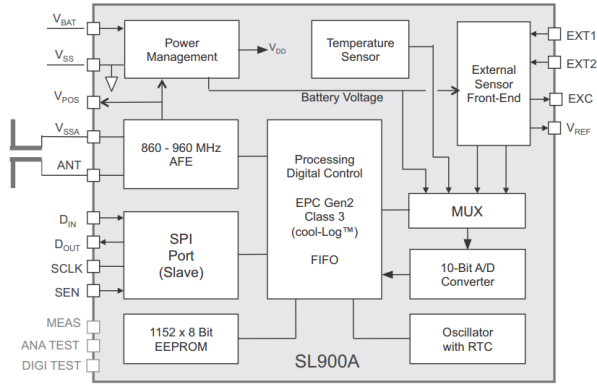


Figure 9. Block diagram of SL900A

The tag chip comprises of some main components: an internal temperature sensor, a SPI interface module for communication data with external MCU (using four signals: Din, Dout, SCLK, and SEN), an external sensor front-end circuit for interfacing with two other external sensors (EXT1 and EXT2), and a power management module that is used to supply voltage from external power in semi-passive mode of the tag. Figure 10 shows the schematic circuit of the proposed tag that can operate in two different strategies, namely, passive mode and semi-passive most. The SPI signals (MISO, MOSI, SCK, SEL) are connected to MCU for receiving ECG data; the battery connector is wired to the RF harvester in semi-passive mode to enhance read range; whereas TP1, TP2 is connected to the tag antenna as shown in Figure 11.

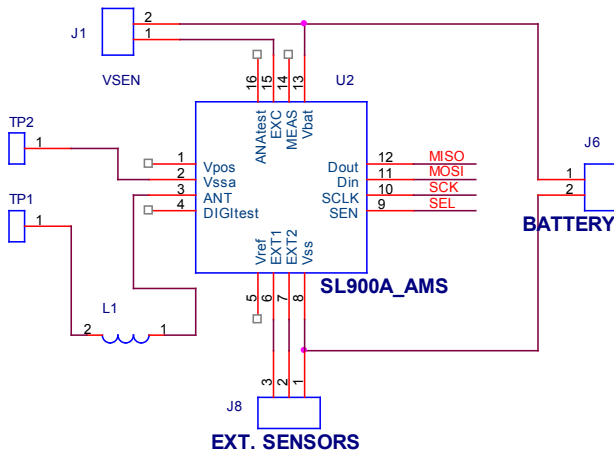


Figure 10. Schematic circuit of the proposed tag

Referring to functions of the SL900A [22], the designed tag antenna has parameters as shown in Figure 11. However, matching inductor (L1) has to be selected to obtain frequency of UHF band for operation of the tag. This study found the best value of 13.4 nH among values from 5.2 nH to 16.4 nH for inductor L1 by using the network analyzer to measure maximum antenna gain at UHF band

(860 MHz ~ 960 MHz) as shown in Figure 12.

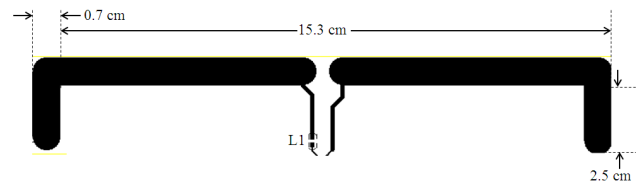


Figure 11. Design of the proposed tag antenna



Figure 12. S11-value of the proposed tag antenna with L1 at 13.4 nH

3.2 MCU, ECG, and Harvester Modules

Figure 13 shows the block diagram for MCU, ECG, and harvester modules. The MCU is created around an extreme low-power microcontroller (PIC16F15xx); the ECG module is based on the ECG circuit that was presented in the next section; whereas the harvester is built around the P1110 (Power Cast Co., USD) that can collect RF energy. In this work, a super-capacitor (C1) whose value is 0.22 F is used to store received power from the harvester. To remain the proposed system in stable operation state, the K-switch is designed to manage the received power. Figure 14 shows the schematic of the K-switch that comprises of a voltage monitor (MAX6264, MAXIM Co.) and a NPN-CMOS transistor. When capacitor voltage is lower a threshold, the K-switch will be off; when the voltage is equal or greater the threshold, the K-switch will be on to supply power to the proposed sensor system.

3.3 The ECG Module

Differences in the speed of wavefront propagation through the cardiac cycle are reflected by different frequencies content of ECG waves. The content of T wave lays mostly within a range from zero (DC) to 10 Hz. The content of P wave is characterized by 5 Hz ~ 30 Hz

frequencies. The content of QRS usually contains within 8 Hz ~ 50 Hz frequencies while abnormal ventricular conduction is characterized by high frequencies (above 70 Hz), forming notches on the QRS. However, the full spectrum of frequencies producing the QRS complex has not been adequately explored. In this study, we chose the frequency of ECG signal from 0.5 Hz to 50 Hz. The proposed ECG circuit is designed using 3 electrodes (LA - left arm, RA - right arm and RLD - GND) as shown in

Figure 15 and Figure 16. The ECG signal obtained from the human body is fed through an IA (Instrument) amplifier, then passed through an HPF (High Pass Filter) filter with a cutoff frequency of 0.2 Hz to filter out baseline noise, then passed to a PA (Power Amplifier) amplifier to increase the signal amplitude, then fed into a 120 Hz LPF (Low Pass Filter) to eliminate high frequency noise before filtering out power line interference using a NF (Notch Filter) to extract the ECG raw signal.

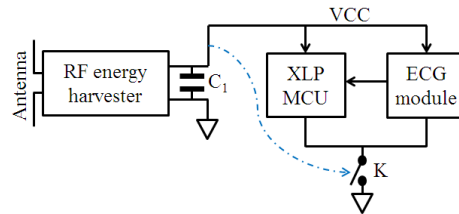


Figure 13. Block diagram of the sensor module with energy harvester

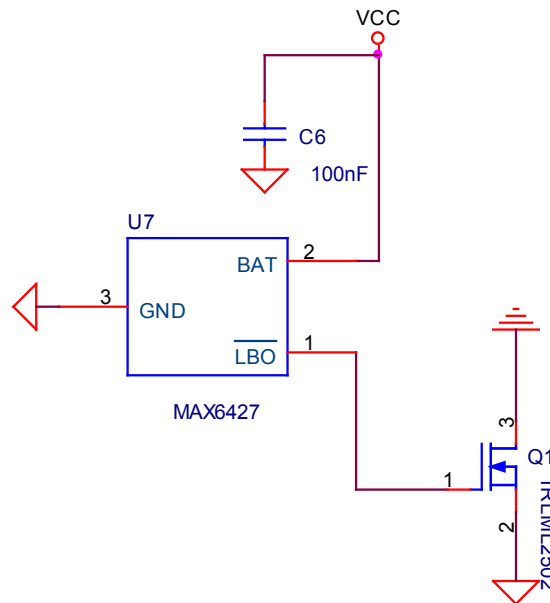


Figure 14. Schematic circuit of the K-switch

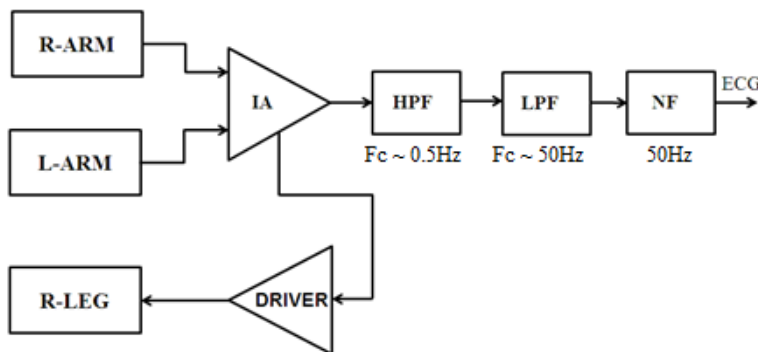


Figure 15. Block diagram of the proposed ECG circuit

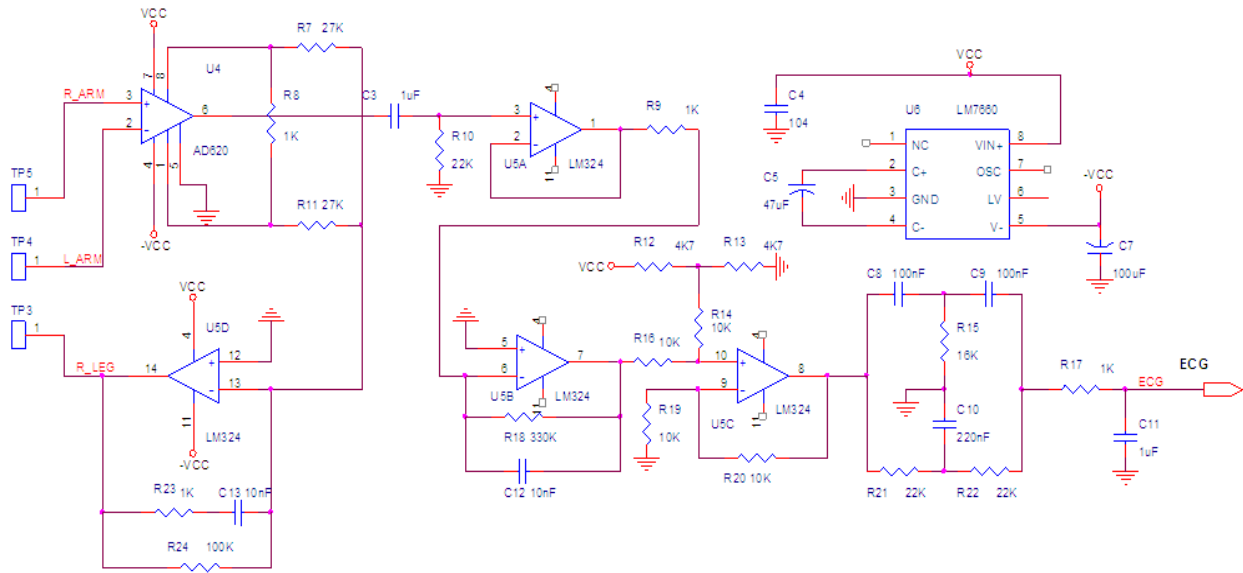


Figure 16. Schematic circuit of the proposed ECG circuit

3.4 The Power Management

The harvesting energy management plays a very important role in voltage distribution to the main power consuming components, the design of which is shown in Figure 17. In this design, the harvested energy is rectified and stored in a 50 mF super capacitor, which is then connected to a 2.1 V voltage lever to close the K1 circuit that powers an MCU. When powered, the MCU controls the power obtained through the voltage divider bridge R1 and R2. When the voltage is enough, the MCU will close K2 to provide the ECG circuit to receive the signal and transmit it to the reader. The harvesting energy control algorithm is shown in Figure 18. When the MCU device is not powered on, the harvester voltage detector checks if $V > 2.1$ V, it will power the MCU, at which point the MCU checks. control energy, when reaching 3.2 V will activate the ECG measuring circuit to work and collect data.

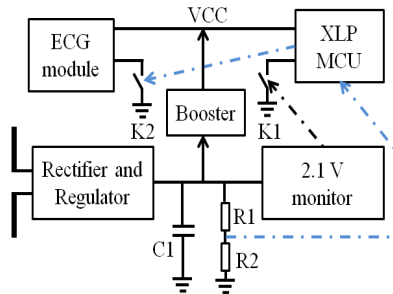


Figure 17. Block diagram of the proposed power manager

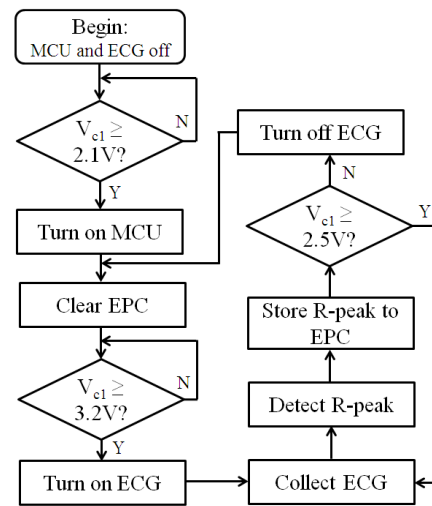


Figure 18. System power controlling

4. Experimental Results

Energy harvesting ECG signal measuring device has been implemented as Figure 19, where Figure 19a is the top side showing upper-capacitor devices (50 mF/5 V) and ECG signal measuring circuit while Figure 19b is the bottom side showing the designed PCB-antenna and the dedicated power harvester, the MCU, the Voltage monitor, and the electrodes. Experimental results are shown from Figure 20 and Figure 21. The results showed that the collected power at distance of 2 m from reader to the proposed ECG sensor. They verified that the proposed system works well with the implemented parameters. The implemented circuit could monitor HRV when it is attached on the human body.

The proposed R-peak detection was coded into the firmware for MCU in the proposed system to detect the peak of the original ECG signals. Figure 22 shows results of the threshold-based method to extract R-peak from ECG raw signal; the results addressed some error peaks due to noise, so that the HRV also have some wrong values (very low val-

ue). Figure 23 shows the results of the proposed algorithm. The results show that premature peaks can be detected. The experimental results highlight the performance of the proposed algorithm under challenge conditions. Therefore the proposed algorithm can be a good solution for real-time R-peak detection in MCU application.

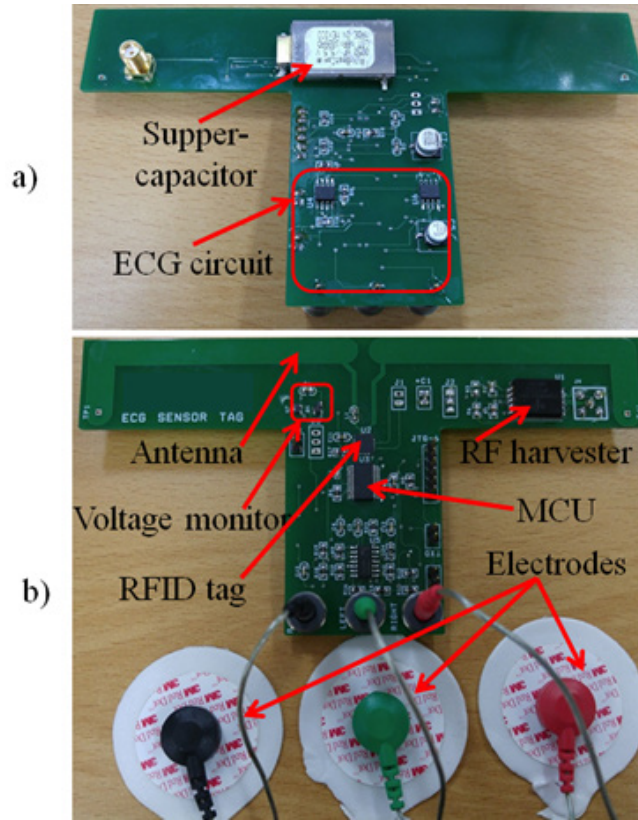


Figure 19. Photograph of the proposed ECG sensor tag; a) top side, b) bottom side

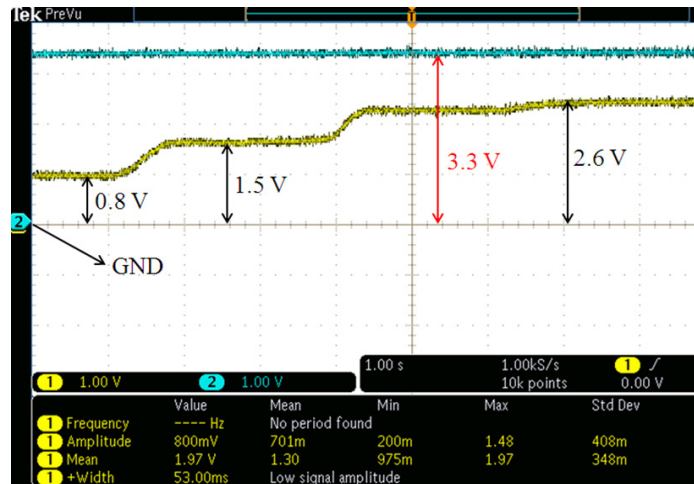


Figure 20. Operation of the boost circuit under various input voltage

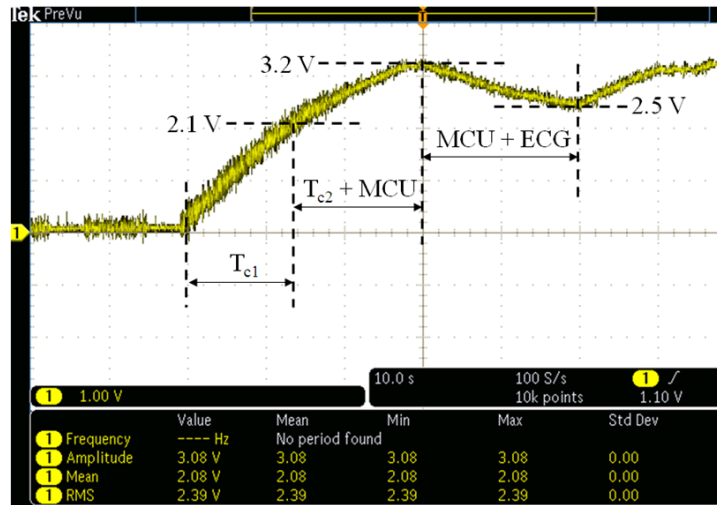


Figure 21. Collected power at distance of 2 m from reader to the proposed ECG sensor tag

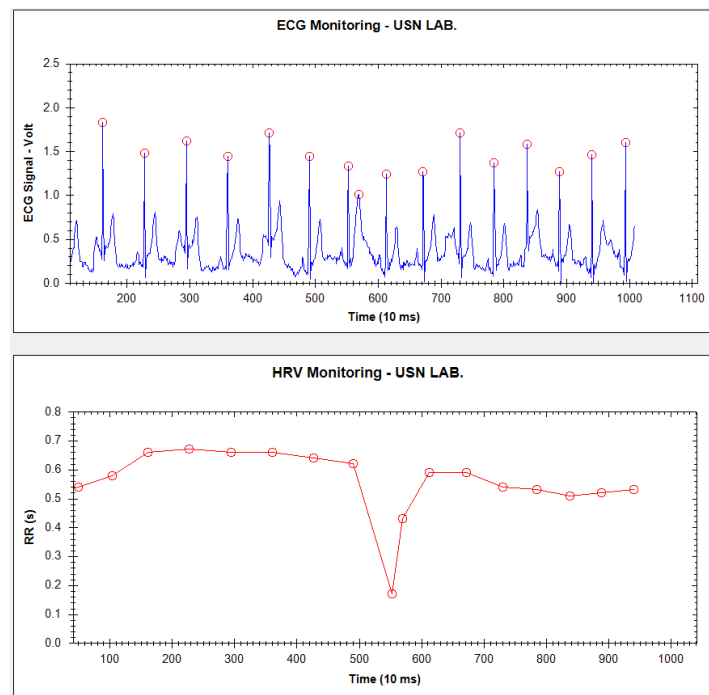


Figure 22. Comparison between R-R and RP for eliminating error peaks

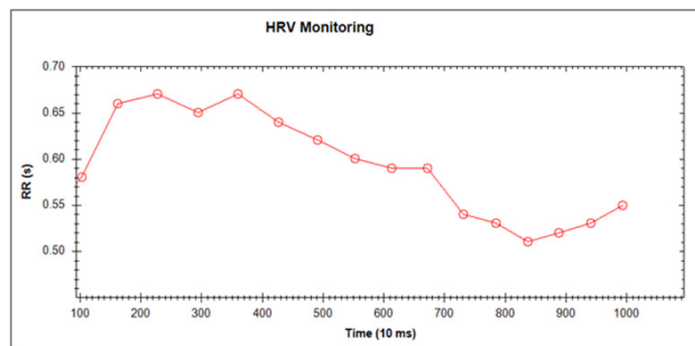


Figure 23. Experimental results of HRV monitoring using the proposed system

5. Conclusions

In this paper, we proposed and implemented a battery less sensing and computational device for monitoring heart rate variability. The implemented system operated well with an ECG circuit that consumes less power of only $\sim 30 \mu\text{A}$ and $\sim 3 \text{ mA}$ on RF harvester at frequency band of 902 MHz \sim 928 MHz. The performance of the proposed system shows that this study can provide a good solution in paving the way to new classes of healthcare applications.

Acknowledgments

This work was supported by FPT University, Hanoi, Vietnam; and Nguyen Tat Thanh University, Ho Chi Minh City, Vietnam.

Conflict of Interest

There is no conflict of interest.

References

- [1] Amini, N., Xu, W., Li, Z., et al., 2011. Experimental Analysis of IEEE 802. 15. 4 for On / Off Body Communications. pp. 2138-2142.
- [2] Choi, J.S., 2010. Performance analysis of ZigBee-based body sensor networks. 2010 IEEE International Conference on Systems, Man and Cybernetics. pp. 2427-2433.
- [3] Dementyev, A., Hodges, S., Taylor, S., et al., 2013. Power consumption analysis of Bluetooth Low Energy, ZigBee and ANT sensor nodes in a cyclic sleep scenario. Wireless Symposium (IWS), 2013 IEEE International. pp. 2-5.
- [4] Andreozzi, E., Sabbadini, R., Centracchio, J., et al., 2022. Multimodal Finger Pulse Wave Sensing: Comparison of Forcecardiography and Photoplethysmography Sensors. *Sensors*, 22, 1-18.
- [5] Jung, S.J., Chung, W.Y., 2011. Flexible and Scalable Patient's Health Monitoring System in 6LoWPAN. *Sensor Letters*. 9(2), 778-785.
- [6] Choi, Y., Zhang, Q., Ko, S., 2013. Noninvasive cuffless blood pressure estimation using pulse transit time and Hilbert-Huang transform. *Computers & Electrical Engineering*. 39(1), 103-111.
- [7] Karmakar, C., Khandoker, A., Penzel, T., et al., 2014. Detection of Respiratory Arousals Using Photoplethysmography (PPG) Signal in Sleep Apnea Patients. *IEEE Biomedical and Health Informatics*. 18(3), 1065-1073.
- [8] Tran, T.V., Chung, W.Y., 2017. A Robust Algorithm for Peak Detection of Photoplethysmograms Waveforms in Mobile Devices. *Journal of Medical Imaging and Health Informatics* 7(7), 1617-1623.
- [9] Alliance, S.B., 1970. Attachment D: RFID Technology Overview. pp. 1-13.
- [10] Salmeron, J.F., Molina-Lopez, F., Rivadeneyra, A., et al., 2014. Design and Development of Sensing RFID Tags on Flexible Foil Compatible With EPC Gen 2. *IEEE Sensors Journal*. 14(12), 4361-4371.
- [11] Dobkin, D., 2007. The RF in RFID: passive UHF RFID in practice. 1.
- [12] RFID standard <http://www.scansource.eu/en/education.htm?eid=12&elang=en>.
- [13] Liao, Y.J., Na, R.T., Rayside, D., 2014. Accurate ECG R-Peak Detection for Telemedicine.
- [14] Rakshita, M., Das, S., 2017. An efficient wavelet-based automated R-peaks detection method using Hilbert transform. *Biocybernetics and Biomedical Engineering*. 37(3), 566-576.
- [15] Chanwimalueang, T., Von Rosenberg, W., Mandic, D.P., 2015. Enabling R-peak Detection in Wearable ECG : Combining Matched Filtering and Hilbert Transform. pp. 134-138.
- [16] Rooijakkers, M., Rabotti, C., Bennebroek, M., et al., 2011. Low-complexity R-peak detection in ECG signals: A preliminary step towards ambulatory fetal monitoring. International Conference of the IEEE Engineering.
- [17] Tran, T., Chung, W.Y., 2015. A Robust Algorithm for Real-Time Peak Detection of Photoplethysmograms using a Personal Computer Mouse. *IEEE Sensors Journal*. 15(c), 1.
- [18] Paper, S., 2009. An Overview of RFID Technology, Application, and Security / Privacy Threats and Solutions.
- [19] Abdulhadi, A., Abhari, R., 2015. Multi-Port UHF RFID Tag Antenna for Enhanced Energy Harvesting of Self-Powered Wireless Sensors. *IEEE Transactions on Industrial Informatics*. 3203(c), 1.
- [20] Rahman, F., Williams, D., Ahamed, S.I., et al., 2014. PriDaC: Privacy Preserving Data Collection in Sensor Enabled RFID Based Healthcare Services. *IEEE International Symposium on High-assurance Systems Engineering*. pp. 236-242.
- [21] A. AMS company, 2014. Data Sheet of the SL900A. pp. 1-90.
- [22] A. AMS company, 2014. RF Characteristics of The SL900A. pp. 1-9.

ARTICLE

Deploying a Deep Learning-based Application for an Efficient Thermal Energy Storage Air-Conditioning (TES-AC) System: Design Guidelines

Mirza Rayana Sanzana^{1*} Mostafa Osama Mostafa Abdulrazic² Jing Ying Wong¹
Chun-Chieh Yip³

1. Department of Civil Engineering, Faculty of Science and Engineering, University of Nottingham Malaysia, Semenyih, Selangor, 43500, Malaysia

2. School of Computer Science, Faculty of Science and Engineering, University of Nottingham Malaysia, Semenyih, Selangor, 43500, Malaysia

3. Department of Civil Engineering, University Tunku Abdul Rahman, Bandar Sungai Long, Cheras, Kajang, Selangor, 43000, Malaysia

ARTICLE INFO

Article history

Received: 29 October 2021

Revised: 24 November 2022

Accepted: 13 December 2022

Published Online: 28 December 2022

Keywords:

Advanced application

Deep learning

Thermal-energy-storage

Air-Conditioner

Facility management and maintenance

Analysis

Design guidelines

ABSTRACT

Facility management and maintenance of the Thermal-Energy-Storage Air-Conditioning (TES-AC) system is a tedious task at a large scale mainly due to the charging load that can increase energy consumption if needed to be charged at peak hours. Besides, maintenance of TES-AC at a large scale gets complex as it contains many sensor data. By utilizing deep learning techniques on the sensor data, charging load prediction can be made possible, so facility managers can prepare in advance. However, a deep learning-based application will be unusable if it is not deployed in a user-friendly manner where facility managers can benefit from this application. Hence, this research focuses on gathering design guidelines for a deep learning-based application and further validates the design considerations with a developed application for efficient human-computer interaction through qualitative analysis. The approach taken to gather design guidelines demonstrated a positive correlation between expert-suggested features and the user-friendly aspect of the application as 67.08% of participants found the features suggested by experts to be most satisfactory. Furthermore, it evaluates user satisfaction with the advanced developed application for TES-AC according to the gathered design guidelines.

*Corresponding Author:

Mirza Rayana Sanzana,

Department of Civil Engineering, Faculty of Science and Engineering, University of Nottingham Malaysia, Semenyih, Selangor, 43500, Malaysia;

Email: sanzanarayana@gmail.com

DOI: <https://doi.org/10.30564/jeis.v4i2.5211>

Copyright © 2022 by the author(s). Published by Bilingual Publishing Co. This is an open access article under the Creative Commons Attribution-NonCommercial 4.0 International (CC BY-NC 4.0) License. (<https://creativecommons.org/licenses/by-nc/4.0/>).

1. Introduction

Global warming has become evident with rising temperatures, heat waves, and hurricanes being felt across the world more ^[1]. Mainly in tropical or subtropical areas, air-conditioning is considered a basic aspect of a building for warm weather conditions. Other than harmful Greenhouse Gas (GHG) emissions, buildings account for around one-fifth of global energy consumption due to the inefficiency of air-conditioning (AC) ^[2,3]. Some major corporations are shifting their focus to a more sustainable form of ac such as thermal storage air conditioning (TES-AC) systems instead of conventional AC units. By using TES-AC, the power consumption of a commercial building along with interrelated costs has been drastically reduced ^[4]. In a tropical country like Malaysia, Air Conditioners (ACs) have the most energy consumption in commercial buildings, and 68.5% savings can be achieved per year by using TES-AC ^[4]. A TES-AC simply works by transferring the charging time from on-peak to off-peak hours and storing the thermal energy to cool buildings for the next day thereby decreasing management costs as well as GHG emissions ^[5]. There are two types of chiller: air-cooled chiller and water-cooled chiller, and a Thermal-Energy-Storage (TES) water-cooled chiller is known to be more energy efficient ^[6]. Yet the companies are hesitant to incorporate TES-AC in commercial buildings as they are concerned about maintenance issues related to tanks not having an optimal volume of water to cool the building during working hours.

A water-cooled chiller has a lot of sensor data which is crucial for Facility Management and Maintenance (FMM) of the TES-AC system. FMM of a building is under the supervision of facility managers, and with the use of digital technologies, Industry 4.0 focuses on efficient building facility handling ^[7,8]. By applying deep learning techniques, such sensor data can be utilized for an efficient FMM as deep learning is essentially a subset of Machine Learning of Artificial Intelligence and is capable of identifying complex patterns in big data i.e., a large dataset with deep layers ^[9,10]. Adopting eco-friendly solutions like TES-AC with a proper maintenance system is important now more than ever to contribute positively to the environment. With deep learning, a smart predictive system to calculate the water volume needed to charge the tanks is possible for optimal water volume prediction for the next day's use considering the external factor of weather temperature ^[11,12]. Although deep learning has a significant role to play in benefiting facility managers mainly in predictive maintenance, the applications of deep learning can be explored further ^[13]. Predictive Maintenance is when

facility managers use computational intelligence to predict a failure, downtime, or maintenance requirements before a failure happens or maintenance is required to lessen downtime and improve building efficiency. According to the study conducted by Sanzana et al. ^[14], Multilayer Perceptron, besides being one of the most common deep learning techniques has demonstrated satisfactory prediction for cooler conditions compared to other common Machine Learning algorithms. Thus, Multilayer Perceptron was preferred for applying deep learning techniques to the TES system to assist facility managers in managing the TES system and is intended to be deployed on the application developed in this study. However, such an advanced system based on deep learning such as Multilayer Perceptron, and Long-Short-Term-Memory, will not be useful to the facility managers if it is not deployed in a proper way for them to utilize it.

Hence, this paper researches the appropriate user-friendly design guidelines for a deep learning-based TES-AC application for efficient human-computer interaction through survey questionnaires for qualitative content analysis. Initially, experts were asked about their preferred features of an advanced FMM application for a water-cooled TES-AC system, and the application was developed accordingly. After that, engineering students were asked about their feedback on the Graphical User Interface (GUI) of the application. The paper aims to find the appropriate design guidelines for an advanced deep learning-based TES-AC application and then to analyze the user-satisfaction in consideration of the suggested guidelines.

2. Literature Review

Human-computer interaction is defined as a way a human interacts with a computer and is a crucial part of designing the GUI of applications. For human-computer interaction research, proper user engagement is a desirable effect and O'Brien et al. ^[15] suggest focusing on disengagement as a necessary human-computer interaction design. There are many challenges in designing graphical user interfaces due to the lack of availability of guidance and targeted experience ^[16]. Various graphical objects, such as cursors, and rendered objects are analyzed in user interaction ^[17]. In advanced applications where there is complex computational intelligence deployed, it becomes even more of a necessity to gather design guidelines so non-experts can benefit from it. Chaudhari et al. ^[18] focus on finding key characteristics of advanced applications for design considerations guidance.

However, in many cases, applications are developed without consulting the target audience which makes the

application cumbersome and not targeted towards the actual needs but solely based on the developer's intuition. Stephanidis^[19] thoroughly discusses the appropriate methods to undergo for developing a computational environment that caters to the preferences, usability, and skills of non-experts as well so an advanced application can be used by the widest user base. Before an advanced application is developed for a specific use, experts can share valuable information such as pointing out which features they would want. This allows for sound development including the necessary features. When there is big sensor data involved, and when deep learning requires high Graphical Processing Units (GPUs), the application needs to be well-planned and useful for the target audience^[9]. Martin-Rodilla et al.^[20] mentioned how suitable interaction techniques are required to understand large data-dependent systems and discuss the challenges faced between human-computer interaction and data analysis applications. Using deep learning techniques, this study suggests improving the usability of the graphical user interface as compared to the manual process of fruit and vegetable identification with Internet-of-Things (IoT)^[21].

Before an application is deployed, it is better to test the user-friendly aspect of the application. It is important to note the way the target audience manages to interact with the application's GUI. A way to test the necessary features is through a survey-based approach as it allows the consumers to outline the desired features through this and this is the reason this research adopted a survey-based approach^[22]. The GUI involves how the application looks, and whether the features in the application manage to execute its actual purpose. It is required to have a methodology that will not let the users be overwhelmed when they are interacting with the GUI and the methodologist can implement new computational methods which will be already integrated into the GUI for ease of use^[23]. It is also important to note if the ambiance, background, fonts, and navigation are not causing any visual disturbance to the users. A dark interface for an application is preferred as it causes less strain on the eyes mainly when it is used for a long. Recently, there has been an increase in the dark user interface trend to reduce ocular diseases of people in continuous use of digital devices^[24]. Yang et al.^[25] suggest a natural user interface to lessen the cognitive load. This study mentions the importance of having a user-friendly environment to run deep learning models^[26]. Underlying human factors are reviewed by Leung et al.^[27] to understand how targeted users may interact with the research area of highlighting techniques. The way users perceive an application is an important evaluation before an appli-

cation is deployed.

3. Materials and Methods

This section will describe the research design adopted for this study in brief and will discuss how the study was conducted. The participants of the study including the questionnaire will be also discussed along with a summarized overview of the application.

3.1 Research Design and Methods

The methodology taken by this research can be viewed in the research framework in Figure 1. There were two different groups of participants, where the initial group consisted of experts in the construction industry, and the latter group involved University students who are pursuing Engineering degrees. Qualitative content analysis is carried out initially by 15 experts to understand the features that will be useful regarding the deep learning-based TES-AC application. After the application is structured based on the suggested features according to the analysis, further analysis is carried out to evaluate the user satisfaction, usability, and interactivity of the application by 35 participants. The participants got a demonstration of the application, and all information they received was in the English Language. No personal information was collected from the participants, and they all were informed about the reasons for the study being conducted before they took part in it. The study had minimal risk and all the participants were adults i.e., 18 years and older. The study was verified to be conducted by the institutional ethics committee.

The following questions were asked in the survey questionnaire for the experts as shown in Table 1. The questions were in Multiple-Choice-Question (MCQ) format in Google Forms for their availability. The MCQ format was chosen so the experts can point out what they prefer within options instead of completely giving them a blank canvas. These questions helped to understand the desirable features and outlook of the application such as whether they want a horizontal or vertical navigation bar. There were also questions to understand whether the experts will find it useful if deep learning is deployed in the predictive maintenance of FMM. Then they were also asked how they would like to view predictions for charging load, statistics related to efficiency, and whether they wanted a "Tips" tab. The experts were also asked regarding the Import feature to upload the sensor data related to TES-AC for charging load prediction and the Export feature to retrieve all the information from the application in a PDF file to view the information.

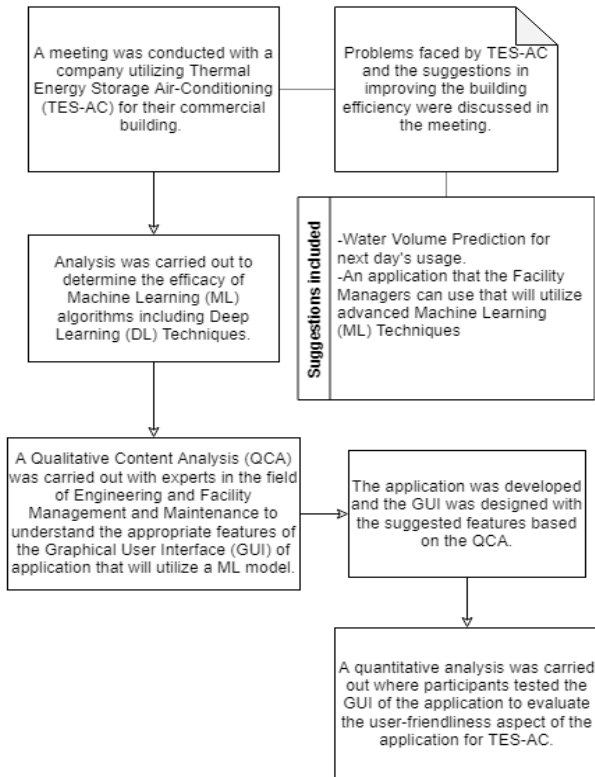


Figure 1. Research Methodology Framework

The following questions as shown in Table 2 were asked to measure the user-interaction aspect of the application to the participants who were pursuing engineering since they might choose to become facility managers. The questions were on a linear scale where 1 denoted least satisfaction and 5 denoted most satisfaction and were available on Google Forms. The questions were designed to understand how they like the overall look of the application, and whether they find a feature easy to use.

3.2 Application Overview

The application has been designed in an untraditional way to make it easier to use and to keep it more interesting. While most maintenance applications would have a very simple design that does not pay attention to details and just places controls and information in front of the user, this application design focused on making an impactful design. The user interface is very easy to use with buttons and text being very clear. The whole application is designed using a science fiction-like theme which makes it more appealing to younger audiences who are most likely to be using this application. It reflects a futuristic design to uplift the mood of the user and relies on visuals and graphics to keep it interesting to look at and boost creativity.

Table 1. Survey questionnaire to understand opinion of experts

| No. | Question description |
|-----|--|
| Q1 | Do you suggest a Login feature for the application so not just anybody gets to view your information? |
| Q2 | For the overall outlook of the application, which option do you suggest will help you to concentrate on your daily activities? |
| Q3 | A navigation bar for the application will allow you to switch to different windows within the application. For the application, do you suggest a horizontal navigation bar or a vertical one? |
| Q4 | This application will be based on a deep learning model for water prediction of Thermal Energy Storage Air-Conditioning (TES AC). Knowing the volume of water needed for the demand of the next day helps improve the building efficiency. Do you believe it will help the facility managers to know the water prediction for the tank? |
| Q5 | Would you want to view the deep learning model-based water volume prediction in a graphical form or just a numerical value? |
| Q6 | A tasking feature will allow you to add tasks and show the completed ones. For better management of TES-AC related tasks, would you suggest the application to have an in-built tasking feature? |
| Q7 | The main reason of water volume prediction is to optimize the energy efficiency of the building. Besides the water volume prediction of the chiller plant, do you also want to view the energy efficiency of your building? |
| Q8 | Do you think displaying the current weather temperature inside the application is useful? |
| Q9 | A lack of interest in upgrading in utilizing deep learning methods are mainly related to many models requiring constant real-time input of sensor data that have specific requirements. Do you suggest that more enterprises will be interested to utilize such advanced deep learning methods if they do not require to change their equipment? |
| Q10 | Would you suggest the application to have an import feature so the .csv dataset files can be used to predict the water volume? |
| Q11 | Do you suggest letting the Facility Managers control the settings for the overall outlook of the application to have a customization aspect? |
| Q12 | Do you think it will be useful to also have an export feature to export the charts and information to a .pdf file for viewing? |
| Q13 | In this TES-AC application, do you think adding a “Tips” tab with helpful information regarding maintenance, or using the application or what certain values depict will make the app better? |

Table 2. Survey questionnaire to evaluate the user-interaction of the application

| No. | Question description |
|-----|--|
| Q1 | Do you like the ambience of the application? |
| Q2 | Do you find the login feature to access the application to be complicated? |
| Q3 | Do you find the overall controls of the application, such as navigating, easy-to-use? |
| Q4 | Do you find the form of water volume prediction easy to understand by looking at the application’s graphical output? |
| Q5 | Do you find the efficiency graphical output to be useful? |
| Q6 | Do you like the customization aspect of the application to control the general settings? |
| Q7 | Do you find changing the control settings of the application easy-to-use? |
| Q8 | Do you find the tasking feature easy-to-use? |
| Q9 | Do you think the “Tips” tab is useful for the users? |
| Q10 | Do you think displaying the current weather temperature is useful? |
| Q11 | Do you think the “Import/Export” tab is a necessary feature for the application? |

As seen in Figure 2 (top), the design of the application relies on a simple but informative interface. The user can easily access the most crucial information and it is easy to navigate the rest of the application. Proper graphics and visuals are used to convey the meaning of the information without the user having to look through manuals to understand what each component of the interface stands for. Figure 2 (bottom) shows how statistics are displayed in the application, using simple graphics that look better than traditional charts but also provide very rich information. A top navigation bar makes it easy to access the different main components of the application while the bottom bar displays information like the time, date, and weather information.

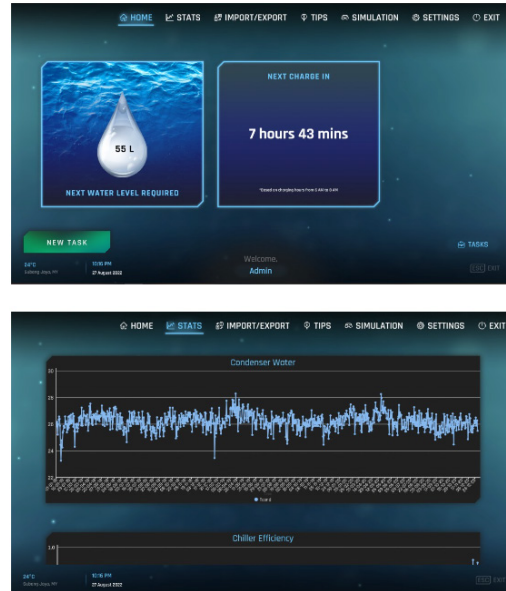


Figure 2. Application snippets

4. Results

According to the QCA, for a user-friendly GUI, the features to include based on experts in the field in the application are displayed in Figure 3. The experts were asked to fill up a survey to understand their desirable features in a deep learning-based facility management application. The participants for the application feature evaluation involved experts aged from 34-60 years (average age 51.8 years), and 14 were males and 1 female. Among 15 experts, 9 were facility managers, 5 were from Civil Engineering and 1 was from Architectural Engineering.

Out of the participants, 86.67% of participants suggested a login feature, 53.33% suggested a futuristic sci-fi background whereas 26.67% wanted a dark background. A total of 73.33% of expert participants wanted a horizontal navigation bar. However, all participants mentioned knowing the charging load required will be useful, and 66.67% wanted to view the information in a graphical form and suggested including a tasking feature. 86.67% of participants also mentioned that viewing energy efficiency statistics will be useful, and 60% of participants said that displaying weather data within the application will be beneficial. When asked if more enterprises will be interested in utilizing advanced technologies such as deep learning if they do not require changing or upgrading their equipment, no participants said no, and 86.67% said that more enterprises will be interested. All the participants wanted an import .csv file feature. 86.67% of participants mentioned that customization of the application would be interesting. Regarding exporting the information displayed

in the application in a pdf file, 86.67% of participants suggested it whereas 13.33% said maybe it will be useful. 80% of participants mentioned including a “Tips” tab as it will be useful for staff.

Among the participants who evaluated the developed application, they were mostly of Civil Engineering background i.e., 20 (68.57%), 5 participants were from Mechanical Engineering background, and 4 participants were from Electrical Engineering background. The age range of participants was between 19-32 years with an average age of 24.66 years. The participants were selected to be young individuals as they will be going for jobs and will handle the chores. Hence their feedback regarding the application interaction was important. As mentioned earlier, the survey was based on a linear scale of 1-5 where 5 exhibited the most satisfaction, and 1 exhibited the least satisfaction. The graphical form of the feedback is shown in Figure 3.

Out of the participants, 19 participants i.e., 54.29% showed the most satisfaction, i.e., scale 5 regarding the ambiance of the application, and 12 participants i.e., 34.29% chose scale 4. Regarding the login feature, no participants found it complicated and found the application controls easy to use. 33 participants i.e., 94.29% chose scale 5 as they found the water volume prediction easy to understand. A total of 29 participants i.e., 82.86% found the graphical efficiency output to be useful, and 30 participants (85.71%) liked the customization aspect of the application. Out of the 35 participants, 25 participants (71.42%) chose scale 5 for changing the controls of the application, and 27 participants (77.14%) found the tasking feature easy to use. Regarding the display of tips for facility management of TES-AC, 19 participants i.e., 54.29% chose a scale of 5. A total of 22 participants

which is 62.86% found the displaying of current weather information within the application to be useful. However, 17 participants (48.57%) found the Import/Export feature to be a necessity for the application as they chose a scale of 5.

To find out if some of the questions’ responses had a significant dependency on the responses of other questions the Chi-square method was used. Using SPSS, the questions that had more than one answer chosen were paired and tested for dependency with other questions. For instance, Q2 asking about the general design of the application retained the null hypothesis with all the other questions confirming that the answers were independent of each other, however, the asymptotic 2-sided p-value was 0.010 with Q9, indicating some sort of relationship between the responses of the two questions. Similarly, Q3 asking about the choice of the navigation bar and Q13 asking about whether to include a Tips section or not had an asymptotic 2-sided p-value of 0.039 indicating that the responses might share a relationship and are somehow interconnected. Moreover, Q5 asking about the choice of visualization for the deep learning model outcome had a significant relationship to Q12 asking about an export feature to export the charts as PDF files. The asymptotic 2-sided p-value here was 0.032. Finally, an asymptotic 2-sided p-value of 0.029 meant that Q11 regarding allowing facility managers to customize the application had a significant relationship with Q13 regarding adding a “tips” feature to the software. All the other question combinations had p-values over 0.05 and therefore retained the null hypothesis which means there are no significant relationships between those questions.

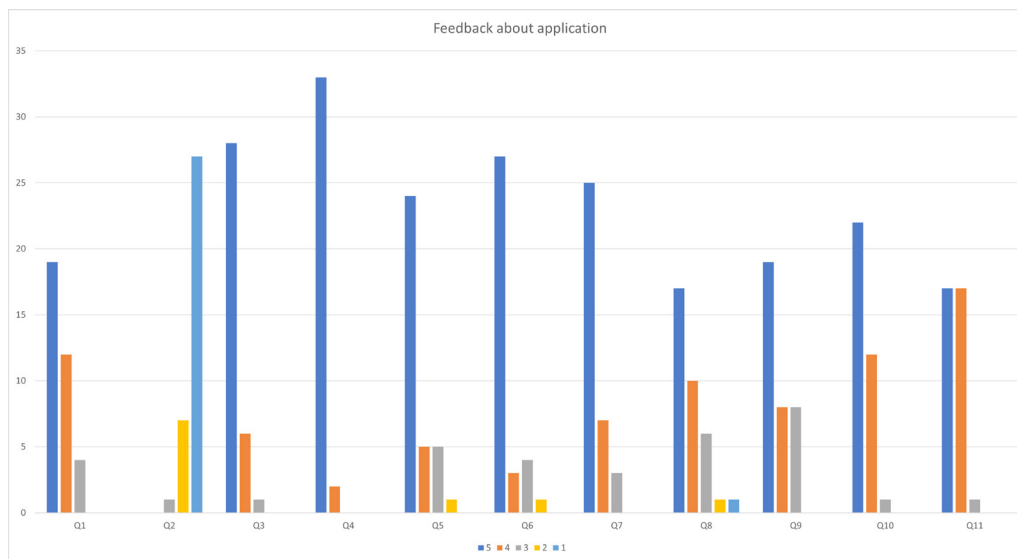


Figure 3. Feedback from the participants on the application

5. Discussion

The facility managers clearly factored in the need for a user-friendly application that can predict the charging load required for the next day's use for the commercial building. As charging load prediction will utilize deep learning, the application needs to be developed with the aspect of user-friendly human-computer interaction. The experts in the facility management field chose certain features to be included in the application. They pointed out that they want a dark futuristic interface for the application which may be because it causes less stress on the eyes. The login feature was suggested by 86.67% as it is an installed desktop application, and it may be useful in data protection. Since 53.33% of experts suggested a futuristic sci-fi background and 26.67% of experts wanted a dark background, the application was developed with a dark futuristic interface. 73.33% of participants wanted a horizontal navigation bar to access the tabs which can be because it is a desktop application, and it is easier to navigate with a horizontal bar. Most of the participants suggested demonstrating energy efficiency statistics and 60% of experts suggested displaying weather data within the application for accessibility reasons. A "Tips" tab was also included according to the suggestion.

When the application was tested for the human-computer interaction aspect by the participants, the overall feedback was positive. This shows initially gathering design guidelines for an advanced application from experts and then developing it is a good approach as it meets the necessary requirements. Among the participants, 88.57% were satisfied with the interface, and 85.71% liked the customization aspect. Also, most of the participants indicated high satisfaction with the user-friendly aspect of switching tabs, using the application, and viewing the predicted charging load and statistics. The participants also appreciated the tasking feature and the accessibility of getting to know the "Tips". Based on the analysis after the demonstration of the application developed, it had the necessary features for the GUI, and the analysis, these design guidelines demonstrated a satisfactory output. To test if the responses to any given question had any significant relationship with the responses to another question, a Chi-square test was applied to the results and while most of the questions retained the null hypothesis and had no significant relationships, four question pairs rejected the null hypothesis and demonstrated having a significant relationship.

5.1 Limitation

The application takes a unique approach in how it was

designed, which resulted in positive feedback, however, it might also result in negative feedback. While most people preferred this type of interface, some users might not be very satisfied with the futuristic design and might prefer a simpler black-and-white interface. This application design would not be very suitable if the users who will be using it prefer the old and traditional way of application designs. It requires the users to be more open to change and willing to adapt.

5.2 Future Direction

The application could be further enhanced by turning it into a website that could be accessed from anywhere so that there is no need to install the application every time on the computers. This allows for better productivity and allows the staff to use the application from home. Moreover, the application could be developed as a phone application which allows the users to have access to it anywhere and at any time. However, developing either of these would be time-consuming, or require professionals to develop it.

6. Conclusions

This research determines the appropriate features to be integrated with a user-friendly GUI for the application for facility management and maintenance of TES-AC that can be used by facility managers and deduces the validity of the human-computer interaction aspect of the application. Furthermore, this study contributes to being a possible approach for gathering design guidelines for an advanced application as the expert suggestions demonstrate satisfaction from the users when included in the application. Among the participants, 67.08% participants found the application developed from the design guidelines collected from the experts to be most satisfactory, which shows the positive correlation measure from expert feedback and user-friendly features. By using the deep learning-based application, facility managers will be able to prepare in advance regarding the charging load, handle the maintenance schedule, allocate tasks, and even prepare for maintenance with suggested tips increasing labor and building efficiency. Also, the design guidelines collected for the deep learning-based application for facility management and maintenance of TES-AC will be beneficial for future researchers and developers who wish to apply computational intelligence for assisting facility managers to make better management decisions through user-friendly software.

Conflict of Interest

Authors declare they do not have any competing interest.

References

- [1] Bryant, C., 2019. Air conditioning is the world's next big threat [Internet]. *The Economic Times*. [Accessed 2020 Jan]. Available from: <https://economictimes.indiatimes.com/news/science/air-conditioning-is-the-worlds-next-big-threat/articleshow/69999842.cms>.
- [2] MacMillan, A., 2016. Global Warming 101. NRDC [Internet] [Accessed 2019 Oct]. Available from: <https://www.nrdc.org/stories/global-warming-101#weather>.
- [3] Ashish, 2022. How Does an Air Conditioner (AC) Work? [Internet] [Accessed 2022 Aug 25]. Available from: <https://www.scienceabc.com/innovation/air-conditioner-ac-work.html>.
- [4] Awang, N.A., Kamar, H.M., Kamsah, N., 2017. Energy saving potential of an air-conditioner-Ice thermal storage (AC-ITS) system. *Journal of Advanced Research in Fluid Mechanics and Thermal Science*. 31(1-10), 1-2.
- [5] Tanks, D., 2015. How Thermal Energy Storage Works [Internet] [Accessed 2022 Aug 22]. Available from: <https://www.dntanks.com/what-we-do/thermal-energy-storage/how-tes-works/>.
- [6] Araner. Difference Between Air Cooled and Water Cooled Chiller System. [Online]. Available from: <https://www.araner.com/blog/difference-between-air-cooled-and-water-cooled-chiller>. [Accessed 30 09 2022].
- [7] Araszkiwicz, K., 2017. Digital technologies in Facility Management - the state of practice. *Creative Construction Conference 2017, CCC 2017, Primošten, Croatia. Procedia Engineering*. 196(2017), 1034-1042.
- [8] Haines, B., 2016. The benefits of lifecycle BIM for facility management [Internet] [Accessed 2019 Nov]. Available from: [https://fmsystems.com/blog/the-benefits-of-lifecycle-bim-for-facility-management/#:~:text=Business%20Information%20Modeling%20\(BIM\)%20has,transformed%20architecture%2C%20engineering%20and%20construction.&text=Facility%20managers%20are%20finding%20value,th](https://fmsystems.com/blog/the-benefits-of-lifecycle-bim-for-facility-management/#:~:text=Business%20Information%20Modeling%20(BIM)%20has,transformed%20architecture%2C%20engineering%20and%20construction.&text=Facility%20managers%20are%20finding%20value,th).
- [9] Education, I.C., 2020. Deep Learning. IBM [Internet][Accessed 2022 Sep 1]. Available from: <https://www.ibm.com/cloud/learn/deep-learning#:~:text=Deep%20learning%20is%20a%20subset,from%20large%20amounts%20of%20data>.
- [10] Mathworks.2022. The mathworks: Deep learning toolbox [Internet] [Accessed 2022 Jan 29]. Available from: <https://www.mathworks.com/products/deep-learning.html>.
- [11] Sanzana, M.R., Abdulrazic, M.O.M., Wong, J.Y., et al., 2022. Effects of external weather on the water consumption of thermal-energy-storage air-conditioning system. *SSRN Electronic Journal*. DOI:10.2139/ssrn.4232763.
- [12] Nguyen, H., Makino, Y., Lim, Y., et al., 2017. Short-term prediction of energy consumption of air conditioners based on weather forecast. 2017 4th NAFOSTED Conference on Information and Computer Science; 2017 Nov 24-25; Hanoi, Vietnam. USA: IEEE. DOI: 10.1109/NAFOSTED.2017.8108063.
- [13] Sanzana, M.R., Maul, T., Wong, J.Y., et al., 2022. Application of deep learning in facility management and maintenance for heating, ventilation, and air conditioning. *Automation in Construction*. 141(9), 104445.
- [14] Sanzana, M.R., Abdulrazic, M., Wong, J.Y., et al., 2022. Analysis of machine learning techniques for predictive maintenance in cooler condition. *The International Symposium on Intelligent Signal Processing and Communication Systems (ISPACS)*; 2022 Nov 22-25; Penang, Malaysia.
- [15] O'Brien, H.L., Roll, I., Kampen, A., et al., 2022. Rethinking (Dis)engagement in human-computer interaction. *Computers in Human Behavior*. 128(3), 107109.
- [16] Lee, C., Kim, S., Han, D., et al., 2020. GUIComp: A GUI design assistant with real-time, multi-faceted feedback. *CHI 20: Proceedings of the 2020 CHI Conference on Human Factors in Computing Systems*; 2020 Apr 23. p.1-13.
- [17] Seinfeld, S., Feuchtner, T., Maselli, A., et al., 2021. User representations in human-computer interaction. *Human-Computer Interaction*. 36(5-6), 400-438.
- [18] Chaudhari, B.S., Zennaro, M., Borkar, S., 2020. LPWAN technologies: Emerging application characteristics, requirements, and design considerations. *Future Internet*. 12(3), 46.
- [19] Stephanidis, C., 2001. User interfaces for all: New perspectives into human-computer interaction. *User Interfaces for All-Concepts, Methods, and Tools*. Lawrence Erlbaum Associates:Hillsdale, NJ. pp. 3-17.
- [20] Martín-Rodilla, P., Panach, J.I., Pastor, O., 2014. User interface design guidelines for rich applications in the context of cultural heritage data. 2014 IEEE Eighth International Conference on Research Challenges in Information Science (RCIS); 2014 May 28-30; Marrakech, Morocco. USA: IEEE.

- [21] Femling, F., Olsson, A., Alonso-Fernandez, F., 2018. Fruit and vegetable identification using machine learning for retail applications. 2018 14th International Conference on Signal-Image Technology & Internet-Based Systems (SITIS); 2018 Nov 26-29; Las Palmas de Gran Canaria, Spain. USA: IEEE.
- [22] Park, C.S., Srinivasan, V., 1994. A survey-based method for measuring and understanding brand equity and its extendibility. *Journal of Marketing Research*. 31(2).
- [23] Wallace, B.C., Dahabreh, I.J., Trikalinos, T.A., et al., 2012. Closing the gap between methodologists and end-users: R as a computational back-end. *Journal of Statistical Software*. 49(5).
- [24] Eisfeld, H., Kristallovich, F., 2020. The Rise of Dark Mode: A qualitative study of an emerging user interface design trend [Internet] [Available from: 2020 Sep 23]. Available from: <http://www.diva-portal.org/smash/record.jsf?pid=diva2%3A1464394&dswid=-2106>.
- [25] Yang, H., Li, J., Han, Y., et al., 2020. Research on the application of new generation of Human-computer interaction in education. 2020 International Conference on Information Science and Education (ICISE-IE); 2020 Dec 04-06; Sanya, China. USA: IEEE.
- [26] Gómez-de-Mariscal, E., García-López-de-Haro, C., Ouyang, W., et al., 2021. DeepImageJ: A user-friendly environment to run deep learning models in ImageJ. *Nature Methods*. 18, 1192-1195.
- [27] Leung, J., Cockburn, A., 2021. Design framework for interactive highlighting techniques. *Foundations and Trends® in Human-Computer Interaction*. 14(2-3), 96-271.



BILINGUAL PUBLISHING CO.
Pioneer of Global Academics Since 1984

Tel.: +65 65881289

E-mail: contact@bilpublishing.com

Website: ojs.bilpublishing.com

2661-3204



9 772661 320223

